

1 **Global Dynamic Molecular Profiles of Stomatal Lineage Cell Development by**
2 **Single-Cell RNA Sequencing**

3 Zhixin Liu^{1†}, Yaping Zhou^{1†}, Jinggong Guo^{1†}, Jiaoai Li^{2‡}, Zixia Tian¹, Zhinan Zhu¹,
4 Jiajing Wang¹, Rui Wu¹, Bo Zhang¹, Yongjian Hu², Yijing Sun², Yan Shangguan²,
5 Weiqiang Li¹, Tao Li², Yunhe Hu², Chenxi Guo¹, Jean-David Rochaix³, Yuchen
6 Miao¹, Xuwu Sun^{1,2*}

7 1 State Key Laboratory of Cotton Biology, Key Laboratory of Plant Stress Biology,
8 School of Life Sciences, Henan University, 85 Minglun Street, Kaifeng 475001,
9 China,

10 2 College of Life Sciences, Shanghai Normal University, Guilin Road 100, Shanghai,
11 200234, China,

12 3 Departments of Molecular Biology and Plant Biology, University of Geneva,
13 Geneva, 1211, Switzerland.

14

15 † These authors have contributed equally to this work.

16 *Correspondence:

17 Contact: Dr. Xuwu Sun

18 State Key Laboratory of Cotton Biology

19 Henan University

20 85 Minglun Street

21 Kaifeng 475001

22 P.R.China

23 sunxuwussd@sina.com

24 Tel: +86 13524016285

25

26

27

28

29

30 **ABSTRACT**

31 The regulation of stomatal lineage cell development has been extensively investigated.
32 However a comprehensive characterization of this biological process based on
33 single-cell transcriptome analysis has not yet been reported. Here, we performed
34 RNA-seq on over 12,844 individual cells from the cotyledons of five-day-old
35 *Arabidopsis* seedlings. We identified 11 cell clusters corresponding mostly to cells at
36 specific stomatal developmental stages with a series of new marker genes.
37 Comparative analysis of genes with the highest variable expression in these cell
38 clusters revealed three transcriptional networks that regulate the development of
39 mesophyll and guard cells, as well as the differentiation from protodermal to guard
40 mother cells. We investigated the developmental dynamics of marker genes via
41 pseudo-time analysis which revealed potential interactions between them. The
42 identification of several novel marker genes suggests new regulatory mechanisms
43 during development of stomatal cell lineage.

44

45

46

47

48

49

50

51

52

53

54

55

56 **INTRODUCTION**

57 Stomata, which are formed by paired guard cells, have played crucial roles in the
58 colonization of land by plants (von Groll and Altmann, 2001). Turgor-driven stomatal
59 movement requires ion and water exchange with neighboring cells and controls
60 transpiration and gas exchange between plants and the environment. To function
61 efficiently, the development of stomata follows a one-cell-spacing rule, in which two
62 stomata are separated by at least one non-stomatal cell (Bergmann and Sack, 2007;
63 Pillitteri and Torii, 2012). In *Arabidopsis*, stomata develop from protodermal cells
64 (PDC) through a series of asymmetrical and symmetrical divisions (Han and Torii,
65 2016). PDCs produce pavement cells (PCs) and self-renewing meristemoids (Ms) that
66 divide asymmetrically several times, generating Ms and PCs known as stomatal
67 lineage ground cells (SLGCs) (Rudall et al., 2013). Ms can eventually differentiate
68 into guard mother cells (GMCs) and a final symmetrical division of a GMC produces
69 two guard cells (GCs) (Geisler et al., 2000). The final spacing between stomata is the
70 result of these M divisions (Pillitteri and Torii, 2012).

71 Several key genes and regulatory networks underlying stomatal development
72 have been uncovered by molecular and genetic analyses. The closely related basic
73 helix-loop-helix (bHLH) transcription factors SPEECHLESS (SPCH), MUTE, and
74 FAMA control sequential cell fate transitions from meristemoid mother cell (MMC)
75 to M, M to GMC, and GMC to GC, respectively (Ohashi-Ito and Bergmann, 2006;
76 MacAlister et al., 2007; Pillitteri et al., 2007). To specify each cell state differentiation,
77 SPCH, MUTE, and FAMA form heterodimers with two paralogous bHLH-leucine
78 zipper (bHLH-LZ) transcription factors, SCREAM (SCRM) and SCRM2 (Kanaoka et
79 al., 2008). In addition, two partially redundant R2R3 MYB transcription factors,
80 FOUR LIPS (FLP) and MYB88, control stomatal terminal differentiation
81 independently of FAMA (GMC to GCs) (Lai et al., 2005; Ohashi-Ito and Bergmann,
82 2006). Two secreted cysteine-rich peptides, EPIDERMAL PATTERNING FACTOR1

83 (*EPF1*) and *EPF2*, are expressed at later and earlier stages of stomatal development,
84 respectively. These peptides are perceived by the cell-surface receptors, ERECTA
85 (ER)-family leucine-rich repeat receptor kinases (LRR-RKs), ER-LIKE1 (*ERL1*) and
86 *ERL2*, resulting in inhibition of stomatal development (Shpak et al., 2005; Hara et al.,
87 2007; Hunt and Gray, 2009b; Lee et al., 2012). The receptor-like protein TOO
88 MANY MOUTHS (TMM) modulates the signaling strength of ER-family receptor
89 kinases in a domain-specific manner (Nadeau and Sack, 2002; Lee et al., 2012).
90 Genetic evidence suggests that these signals are mediated via a mitogen-activated
91 protein kinase (MAPK) cascade, which eventually downregulates the transcription
92 factors responsible for initiating stomatal lineage via direct phosphorylation
93 (Bergmann et al., 2004; Lampard et al., 2008; Lampard et al., 2009; Kim et al., 2012).
94 Stomagen (also known as EPF-LIKE9) peptide promotes stomatal development by
95 competing with EPF2 for binding to ER (Sugano et al., 2010; Zhang et al., 2014;
96 Hronkova et al., 2015). One homeodomain-leucine zipper IV (HD-ZIP IV) protein,
97 HOMEODOMAIN GLABROUS2 (HDG2), acts as a key epidermal component
98 promoting stomatal differentiation (Peterson et al., 2013). It is highly expressed in
99 meristemoids, and a *hdg2* mutant exhibits delayed meristemoid-to-GMC transition
100 (Peterson et al., 2013).

101 Gene expression profiles for different types of stomatal lineage cells are
102 currently lacking, resulting in a poor understanding of the regulatory mechanisms
103 controlling the PDC to MMC transition. To gain new insights into this process, we
104 isolated protoplasts from cotyledons of five-day-old *Arabidopsis* seedlings for
105 single-cell RNA sequencing (scRNA-seq). We classified the major cell types and
106 employed transcriptomic analysis to identify several potential key regulators and
107 signaling pathways present in these heterogeneous cell populations. Our analysis led
108 to the identification of a regulatory network of transcription factors for specific
109 developmental stages of stomatal lineage cells. Pseudo-time analysis was employed to
110 uncover the interactions and mutual regulation among key marker genes at different
111 developmental stages. We also identified several novel marker genes that play
112 important roles in regulating stomatal development. These results provide insights
113 into how single-cell transcriptomics can be used to further elucidate the regulatory
114 mechanisms controlling the differentiation of stomatal lineage cells.

115 **RESULTS**

116 **Gene Expression Pattern of Stomatal Lineage Cells**

117 To systematically resolve gene expression patterns in specific stomatal lineage cells at
118 different developmental stages, we prepared protoplasts by enzymatic digestion from
119 the cotyledons of five-day-old seedlings. The protoplasts were screened with a 40 μ m
120 pore cell strainer to obtain more than 20,000 individual cells. Single cells were
121 labeled using 10 \times Genomics barcode technology, followed by reverse transcription to
122 obtain a single cell cDNA library (Figure S1). This cDNA library was utilized for
123 high throughput sequencing (Figure S1). After extensive analysis of the sequencing
124 results, we obtained transcriptome information for 13,999 single cells (Figure S2). We
125 also identified mitochondrial (mito), chloroplast (pt) and ribosomal (ribo)
126 transcriptomes. Transcripts from these subcellular organelles were excluded from
127 subsequent analysis, resulting in 12,844 single-cell transcriptomes that were further
128 analyzed. They were classified into 11 clusters using t-distributed stochastic
129 neighborhood embedding (t-SNE) (Figure 1). We selected representative marker
130 genes to identify each different cell type: for mesophyll cells (MPC), we used
131 *Ribulose Bisphosphate Carboxylase Small Subunit (RBCS)* and *light-harvesting*
132 *chlorophyll a/b-binding protein (LHCB)* as markers that encode chloroplast proteins
133 and are high expressed in MPC; for the epidermal cell populations, we selected *EPF2*,
134 *BASL*, *TMM* and *SPCH* as markers for PDC (Pillitteri and Dong, 2013); *POLAR*,
135 *SPCH*, *TMM*, *MUTE*, *HDG2* and *EPF2* were used for MMC (Pillitteri and Dong,
136 2013); *MUTE*, *BASL*, *SPCH* and *EPF2* were selected for early stage meristemoid (EM)
137 cell identification (Pillitteri and Dong, 2013); *BASL*, *MUTE* and *EPF1* were chosen
138 for late stage meristemoid (LM) cells, while *EPF1*, *HIC*, *FAMA* and *SCRM* were used
139 for GMC (Pillitteri and Dong, 2013); *RBCS*, *FAMA* and *EPF1* were utilized for young
140 guard cells (YGC) (Pillitteri and Dong, 2013); high expression of *HIC*, *RBCS*, *FAMA*
141 combined with low expression of *EPF1* and *EPF2* was used as a marker for GC
142 (Pillitteri and Dong, 2013); *ROP2*, *ROP6*, *ARP2*, *ARP3*, *IQD5* and *RBCS* for PC (Xu
143 et al., 2011; Zhang et al., 2013; Barton et al., 2016; Liang et al., 2018). Because there
144 are chloroplasts in GC, YGC and PC, we also used *RBCS* as marker for these cells
145 (Barton et al., 2016).

146 The expression profiles of the above selected marker genes have been
147 determined previously. *SPCH* is expressed in the developing leaf epidermis
148 (MacAlister et al., 2007). A transcriptional green fluorescent protein (GFP) reporter
149 (*SPCHpro::nucGFP*) and a translational reporter (*SPCHpro::SPCH-GFP*) are
150 expressed in a subset of epidermal cells that lack overt signs of differentiation
151 (MacAlister et al., 2007). In cotyledons, *SPCH* expression is often observed in two
152 neighbouring cells, a pattern consistent with expression in the dividing cell population
153 (MacAlister et al., 2007). In older organs, *SPCHpro::SPCH-GFP* expression
154 continues to be restricted to small cells in the epidermis, including cells that have
155 recently divided next to stomatal lineage cells (MacAlister et al., 2007). In
156 meristemoids, *SPCH* expression is downregulated and *MUTE* expression commences
157 (MacAlister et al., 2007). *MUTE* is required to limit the number of rounds of
158 meristemoid division and expressed strongly in meristemoids and at lower levels in
159 GMCs and GCs (Pillitteri et al., 2007). *FAMA* is expressed in GMCs and is necessary
160 and sufficient to promote GC identity (Ohashi-Ito and Bergmann, 2006). The
161 *PROFAMA:GFP* expression is restricted to the stomatal lineage (Ohashi-Ito and
162 Bergmann, 2006). The *PROFAMA:GFP* is not expressed in meristemoids but is
163 strongly expressed in GMCs and in YGCs (Ohashi-Ito and Bergmann, 2006). *BASL*
164 and *POLAR* show largely overlapping localization at the cell cortex during stomatal
165 asymmetric divisions (Dong et al., 2009). In the cotyledon and leaf epidermis,
166 *BASL::GUS* is highly expressed in the asymmetrically dividing MMCs and
167 meristemoids, and it is undetectable in later stomatal lineage cells (Dong et al., 2009).
168 *ProTMM::TMM-GFP* is expressed in proliferating stomatal lineage cells, but not in
169 other epidermal cells or in mature stomata (Nadeau and Sack, 2002). *EPF2* is
170 produced in *SPCH*-expressing PDC (MMCs) early in the lineage, whereas *EPF1* is
171 produced in late-stage meristemoids, GMCs and young guard cells (Hara et al., 2007;
172 Hunt and Gray, 2009a). Consistent with the report on *HDG2pro::GUS* (Nakamura et
173 al., 2006), the GFP signals of the *HDG2* transcriptional reporter
174 (*HDG2pro::nls-3xGFP*) are strongly expressed in meristemoids and SLGCs (Peterson

175 et al., 2013). The HDG2 translational reporter (*HDG2pro::HDG2-GFP*) accumulates
176 in the nuclei of meristemoids and SLGCs (Peterson et al., 2013). ROP2 and ROP6 are
177 locally activated at the opposing sides of the cell wall and are mutually exclusive
178 along the plasma membrane within PCs (Fu et al., 2005; Xu et al., 2011). In addition,
179 microtubule-associated protein IQ67 DOMAIN 5 (IQD5) is localized in PC (Liang et
180 al., 2018). The *GFP:IQD5* colocalizes with the microtubule marker *mCherry:TUB6*
181 (mCherry fused to β -tubulin6) in both leaf PC and hypocotyl epidermal cells (Liang et
182 al., 2018). The scheme in Figure 1A, B displays the expression pattern of selected
183 marker genes in different stomatal cell types.

184 **Identification of the cell types with marker genes**

185 To determine the cell type with the above marker genes, we analyzed the pattern of
186 selected marker genes in each cell cluster. As shown in Figure S3A and B, *FAMA*
187 expression is high in clusters 6 and 7. *SCRM* is expressed in clusters 6,7,8 and 10
188 (Figure S3A and B). *SPCH* expression is high in clusters 7,8 and 9 (Figure S3A).
189 *MUTE* is expressed in cluster 8 (Figure S3A). *BASL* is expressed in clusters 1, 4 and
190 10 (Figure S3A). High expression of *POLAR* is found in clusters 6, 7 and 8 (Figure
191 S3A). *EPF1* is expressed in clusters 6, 7 and 8, while *EPF2* is expressed in clusters 6,
192 7, 9 and 10 (Figure S3A). *EPFL9*, *ROP2*, *ROP6* and *IQD5* are highly expressed in
193 cluster 0 (Figure S3A). Based on the expression patterns of these marker genes, we
194 can determine the cell type of each cluster as follows: cluster 0 is PC, cluster 1 is PDC,
195 cluster 8 is MMC, cluster 3 is EM, cluster 4 is LM, cluster 10 is GMC, cluster 7 is
196 YGC and cluster 6 is GC (Figure 1C). The expression of *RBCS* and *PSAB* is mainly
197 enriched in clusters 2 and 5 indicating that they correspond to MPCs. To distinguish
198 them, we named them MPC_2 and MPC_5 respectively (Figure 1C). For cluster 9, we
199 could not determine its cell type with the known marker genes. However amongst the
200 genes that belong to this cluster, we checked the stomatal pattern in the corresponding
201 mutants. As an example we found that *BCL-2-ASSOCIATED ATHANOGENE 6* (*bag6*)
202 affects the distribution of GC and produces some double and adjacent GCs, as well as

203 an increase of SI compared with WT (Figure 1A, Figure S4). Plant BAG proteins are
204 homologs of mammalian regulators of apoptosis and play important roles in
205 regulating apoptotic-like processes ranging from pathogen attack, to abiotic stress, to
206 plant development (Kabbage and Dickman, 2008; Li et al., 2016; Fu et al.,
207 2019). Expression of *BAG6* in leaves was strongly induced by heat stress (Fu et al.,
208 2019). Loss of function of *BAG6* in *fes1a bag6* double mutant partially rescued the
209 sensitive of *fes1a* to heat stress (Fu et al., 2019). The *bag6* mutant shows enhanced
210 susceptibility to the fungal pathogen *Botrytis cinerea*, both in terms of severity of
211 lesions and rate of spread (Li et al., 2016). Since stomata are important entry sites for
212 fungal pathogens (Melotto et al., 2006; Underwood et al., 2007; Dutton et al., 2019;
213 Zhang et al., 2019), the increased number of stomata in *bag6* may lead to the fast
214 spread of *Botrytis cinerea*. Another mutant from cluster 9 marker genes, *bzip6*, does
215 not significantly affect the development of stomata. The expression of
216 *bZIP6::ER-GFP* occurs specifically in two pericycles in the phloem pole starting
217 from the early root elongation zone (Lee et al., 2006) . These results suggest that
218 *bZIP6* is not a marker gene of stomata. and that cluster 9 does not belong to epidermal
219 cells although the *bag6* mutant is defective in the distribution of GC.

220 To investigate the abundance of gene transcripts in different cell types, we
221 counted the number of cells and the number of transcripts identified in each cell type
222 (Figure S5A and B and Supplemental Table S1). Note that the number of different
223 cell types identified here does not directly reflect the relative number of different cell
224 types in the cotyledons of plants. The number of identified cells only reflects the
225 relative number of each cell type in the cell samples we obtained. At the same time,
226 the number of transcripts identified in each cell type was also quantitatively analyzed
227 by determining the average number of transcripts identified in each cell for
228 comparison (Figure S5C). The results show that the number of average transcripts in
229 PC was lowest, whereas it was highest in GMC. In contrast, a relatively high number
230 of transcripts was identified in MMC, PDC and EM (Figure S5C).

231 **Expression of marker genes in stomatal lineage cells**

232 To further test the cell type that we identified, we analyzed the expression of several
233 known marker genes that are involved in regulating the development of stomatal
234 lineage cells. As shown in Figure S3B, *FAMA*, *TMM*, *HIC* and *SCRM* are specifically
235 expressed in YGC and GMC, while other marker genes are not only expressed in
236 YGC and GMC, but also in other cell types (Figure S3B), suggesting that their
237 functions may not be only restricted to the regulation of stomatal lineage cell
238 development. To explore the potential regulators of stomatal lineage cells, we
239 analyzed gene expression profiles in different clusters and identified highly expressed
240 marker genes in each individual cell cluster (Figure 2A). Feature plot analysis
241 indicated that the expression of newly identified marker genes is clearly increased in
242 their corresponding clusters (Figure 2B and Supplemental Table S2). Some of these
243 marker genes could potentially be involved in regulating the development of stomatal
244 lineage cells. *SLAC1* and *SCAP1*(*DOF5.7*) play important roles in regulating the
245 development of stomatal lineage cells (Engineer et al., 2015; Chen et al., 2016).
246 Consistently, a high level of expression of *SLAC1* and *DOF5.7* was detected in YGC
247 and GMC (Figure 2A). Furthermore, a pectin methylesterase gene, *PME6*, is highly
248 expressed in YGC and GMC (Figure 2A). As reported, *PME6* is highly expressed in
249 guard cells and required for stomatal function (Amsbury et al., 2016). Guard cells
250 from *pme6-1* mutant have walls enriched in methyl-esterified pectin and show a
251 decreased dynamic range in response to elevated osmoticum, suggesting that the
252 mechanical change in the guard cell wall can affect stomatal function (Amsbury et al.,
253 2016). The *Arabidopsis* K^+ channel gene, *KAT2*, is expressed in guard cells (Pilot et
254 al., 2001). *KAT2* is a major determinant of the inward K^+ current through the guard
255 cell membrane (Pilot et al., 2001). Interestingly, the expression of *ARABIDOPSIS*
256 *THALIANA MERISTEM LAYER1*(*ATML1*) was high in MMC, where the established
257 marker genes *SPCH* and *MUTE* were also highly expressed (Figure 2A).

258 In GC, we identified 10 top marker genes that may be involved in regulating the
259 function of GC (Figure 2A). Stomata are not only required for gas exchange with the
260 environment and for controlling water loss, but they also provide routes for pathogen

entry into plants (Zeng et al., 2010). Therefore plants have evolved mechanisms to regulate stomatal aperture as an immune response against bacterial invasion (Zeng et al., 2010). A recent study showed that bacterial infection can induce systemic signaling to inhibit the development of stomata in new leaves to restrict pathogen entry (Dutton et al., 2019). The bacterial peptide flg22 or the phytohormone salicylic acid (SA) induce a similar systemic decrease in stomatal density (Dutton et al., 2019). This developmental process can be regulated by AZELAIC ACID INDUCED 1 (AZI1), which is involved in the priming of SA induction and systemic immunity triggered by pathogen or azelaic acid (Pitzschke et al., 2016). *KTII* encodes an *Arabidopsis* serine protease (Kunitz trypsin) inhibitor and plays important roles in modulating PCD in plant-pathogen interactions (Li et al., 2008). Expression of *AtKTII* is induced late in response to bacterial and fungal elicitors and to salicylic acid (Li et al., 2008). Besides SA, camalexin is also involved in regulating the defense response of plants. One of cytochrome P450 enzymes, CYP71A12 is an important component in the biosynthetic pathway of camalexin and related metabolites (Mucha et al., 2019). Pathogen infection can induce the expression of *CYP71A12*, which leads to dehydration of IAOx to form indole-3-acetonitrile (IAN) during the biosynthesis of camalexin (Nafisi et al., 2007; Muller et al., 2015). CYP71A12 is involved in the biosynthetic pathway to 4-hydroxyindole-3-carbonyl nitrile (4-OH-ICN), the level of all ICN derivatives with the exception of A6 in *cyp71a12* mutant is about 10% of WT (Rajniak et al., 2015). 4-OH-ICN plays roles in inducing the pathogen defense (Rajniak et al., 2015). *CYP71A12* is co-expressed with a flavin-dependent oxidoreductase 1 (*FOX1*), and levels of ICN metabolites in the *fox1* mutant are decreased three- to fivefold compared with WT (Rajniak et al., 2015).

Consistent with these findings, *KT1*, *CYP71A12* and *FOX1* are expressed in GC (Figure 2A) further supporting that stomatal cells may fight against pathogens by producing IAN and OCN. Opening of stomata in response to various stimuli is regulated by K^+ uptake through inward-rectifying K^+ channels in the plasma membrane (Szyroki et al., 2001). *CHX17* encodes a putative K^+/H^+ exchanger.

290 *CHX17* cDNA complements the phenotypes of the *khalDelta* mutation in *S.*
291 *cerevisiae* cells, which shows a growth defect at increased pH and hygromycin
292 sensitivity (Maresova and Sychrova, 2006). Under its native promoter,
293 AtCHX17(1-820)-GFP is localized in the prevacuolar compartment and in plasma
294 membrane in roots (Chanroj et al., 2013). Expression of *CHX17* in GC suggests that it
295 may be involved in regulating the opening of stomata.

296 **ATML1 is involved in regulating the development of stomatal lineage**
297 **cells**

298 To explore the potential regulator of MMC, we analyzed the marker genes in MMC
299 and found that *ATML1*, *PDF1*, *MUTE* and *SPCH* have highly similar expression
300 profiles (Figure 2A and Figure S3A). To investigate the roles of ATML1 in the
301 regulation of epidermal cell differentiation, Takada et al generated a construct
302 *proRPS5A-ATML1* that uses the promoter region of *AtRPS5A* to drive the expression
303 of *ATML1* (Takada et al., 2013). The resulting construct was transformed into a
304 transgenic plant containing *STOMAGEN-GUS* to investigate the effects of ATML1 on
305 the expression of the mesophyll-specific *STOMAGEN-GUS* reporter (Takada et al.,
306 2013). In the transgenic plants of *proRPS5A-ATML1*, the expression of *ATML1* was
307 induced by treating the seedlings with β-estradiol (Takada et al., 2013).
308 Overexpression of *ATML1* induced stomata-like structures in the inner cells of the
309 cotyledons in independent lines (Takada et al., 2013). These ectopic guard cell-like
310 cells expressed the guard cell marker *KAT1-GUS*, suggesting that these cells have
311 guard cell identity (Takada et al., 2013). This result also suggested that overexpression
312 of *ATML1* can induce the development of stomata. Moreover, induction of *ATML1*
313 can inhibit the expression of mesophyll-specific *STOMAGEN-GUS* and result in
314 miss-shaped leaves with ectopic patches of transparent cells among the green
315 mesophyll tissues (Takada et al., 2013). These results suggest that induction of
316 *ATML1* can enhance the biogenesis of stomata but inhibit the development of
317 mesophyll tissues. Although *STOMAGEN* can enhance the biogenesis of stomata

318 (Lee et al., 2015), induction of *ATML1* does not inhibit the biogenesis of stomata even
319 if the expression of *STOMAGEN* is suppressed by *ATML1*, suggesting that *ATML1*
320 may rely on a *STOMAGEN*-independent pathway to enhance the biogenesis of
321 stomata. Furthermore, the SI of the *atml* mutant is decreased, while the SI of
322 *ATML1*-OX transgenic plant overexpressing *ATML1* is increased (Peterson et al.,
323 2013), suggesting that *ATML1* is involved in regulating the development of stomata.
324 To investigate the effects of *ATML1* on the biogenesis of stomatal lineage cells, we
325 used mutants of *ATML1*. As expected, *atml1-2* and *atml1-3* plants are deficient in the
326 development of stomatal lineage cells (Figure 3A-F). Further RT-PCR analysis
327 indicated that the expression levels of *SPCH* and *MUTE* in *atml1-2* and *atml1-3* were
328 lower than in WT (Figure 3G), suggesting that *ATML1* can regulate the development
329 of stomatal lineage cells by modulating the expression of both *SPCH* and *MUTE*.

330 **GO Analysis of the genes enriched in different cell types**

331 To investigate the potential biological function of genes expressed in each cell type,
332 we performed GO analysis on all cell clusters (Figure 4 and Figure S6). There were
333 significant differences in the number of enriched genes identified in different cell
334 types. In general, the majority of enriched terms were associated with individual cell
335 types, however those GO terms associated with multiple cell types represent more
336 general biological processes (e.g., response to oxidative stress and salt stress, and
337 vesicle-mediated transport) (Figure 4A and Figure S6). As a measure of the reliability
338 of our method in identifying cell type-expressed genes and of our ability to correctly
339 annotate biological processes to a cell type, we compared a list of genes enriched in
340 GCs in our analysis with a previous study that profiled GC functions. In agreement
341 with these published reports (Gray, 2005; Lawson, 2009; Song et al., 2014; Niu et al.,
342 2018; Huang et al., 2019), we found genes that respond to oxidative stress, salt stress,
343 bacteria, cadmium ions and are involved in stomatal movement and photosynthesis,
344 are preferentially expressed in GCs (Figure 4A and Figure S6). Our analysis further
345 increased the spectrum of biological processes associated with GC development to

346 include protein transport, vesicle-mediated transport, and cell death (Figure 4A and
347 Figure S6). Since this result indicated that our method is suitable, we used gene
348 categories that are preferentially expressed to infer the function of other cell types.
349 Gene ontology (GO) heatmap analysis indicated that the genes expressed in PC and
350 MPC are mainly involved in photosynthesis and carbohydrate metabolism (Figure
351 4A). The genes with increased expression in GCs and YGCs are also involved in
352 photosynthesis, which is consistent with the presence of chloroplasts in these cells
353 (Figure 4A). The genes expressed in cluster 9 are mainly implicated in the response to
354 abiotic and biotic stress and protein transport (Figure 4A). We could not assign a cell
355 type to cluster 9 due to the uncertainty about marker genes (Figure 4A). GO heatmap
356 analysis revealed that MMC, EM, LM and GMC are similar (Figure 4A and B). In
357 these cells, the expressed genes are not involved in photosynthesis (Figure 4A).
358 Unexpectedly, we found that genes preferentially expressed in these cells are involved
359 in regulating the response to all kinds of environmental stress and stimulus (Figure 4A
360 and B and Figure S6). For instance, genes that respond to bacteria are highly
361 expressed in MMC (Figure 4B). Compared with LM and GMC, the most important
362 feature of MMC is the lack of gene expression associated with the respiratory chain
363 and oxidative phosphorylation (Figure 4B), suggesting that MMCs have relatively
364 low metabolic activity. However, genes enriched in PDC and MMC are involved in
365 protein transport, vesicle-mediated transport and membrane protein complexes
366 (Figure 4A and Figure S6), suggesting that PDC and MMC show higher activity of
367 protein expression.

368 **Analysis of the regulatory network of transcription factors (TFs) in
369 different cell types**

370 To investigate the mechanisms that regulate the development of different cell types,
371 we analyzed the regulatory network of TFs in each of them. We first analyzed the
372 number of TFs in different cell types, as shown in Figure 5A. In PDC, we identified
373 the highest number of TFs, while in MPC_5, we identified the lowest number of TFs.
374 More TFs were identified in EM, LM, MMC and GMC, but less in GC and YGC.

375 Accumulation of TFs in PDC, EM, LM, MMC and GMC showed that gene
376 expression was higher at the early stage of development of stomatal cells, and the
377 number of TFs needed was also higher. In GC and YGC, gene expression was
378 relatively low. Surprisingly, we found that the number of TFs in MPC_2 and MPC_5
379 was lower than in other cell types. Although MPCs are important for photosynthesis
380 and for a series of important metabolic reactions, their gene expression is relatively
381 low. This is consistent with the low average number of highly expressed genes in
382 MPC cells (Figure S5A and B). The mRNAs of the transcription factors (TFs) *BASIC*
383 *PENTACYSTEINE1(BPC1)*, *BPC6*, and *WRKY33* are highly expressed in PC and
384 MPC (Figure 5A). We further analyzed the regulatory network of these TFs by
385 analyzing the genes co-expressed with them and extracted the top 1,000 links showing
386 positive correlation with BPC6 and WRKY33 (Figure 5A). We found that BPC6 and
387 WRKY33 are core TFs in regulating the development and function of PC and MPC
388 (Figure 5A). Analysis of the regulatory network of TFs in YGC and GC suggests that
389 BPC1, BPC6 and SCRM may act as the core TFs regulating the development and
390 function of PC and GC (Figure 5B). SCRM has been shown to interact with FAMA to
391 regulate the differentiation from GMC to GC (Kanaoka et al., 2008). Thus, our results
392 suggest that BPC1 and BPC6 may mediate the development of GC in conjunction
393 with SCRM. Analysis of the regulatory network of TFs in MMC, EM, LM and GMC
394 indicates that they have fewer close interactions with known transcription factors
395 (except for SCRM, SPCH and SCRM2), but they are all associated with *BPC1* and
396 *BPC6* based on co-expression (Figure 5C). There is also a close regulatory
397 relationship between BPC1 and BPC6, which form the core of the transcriptional
398 regulatory network in these cell types (Figure 5C). This finding suggests that BPC1
399 and BPC6 may regulate the differentiation from PDC to GMC by interacting with
400 other transcription factors. Furthermore, we also found that PIF5, BPC1, BPC6,
401 WRKY33, ATML1, and SCRM can act as core TFs to regulate the differentiation
402 from PDC to GMC (Figure 5D). Feature plot analysis indicated that expression of
403 *BPC1*, *BPC2*, *BPC4* and *BPC6* is mainly enhanced in MMC, EM, LM, GMC, YGC
404 and GC, while the expression of *WRKY33* can be detected in all cell types (Figure 6A).
405 Analysis of the stomatal developmental pattern indicated that the number of GC in
406 *wrky33* is decreased, while the numbers of M and GMC in *wrky33* are increased,

407 compared with WT (Figure 6B and C), suggesting that WRKY33 is involved in
408 regulating the development of GC from GMC.

409 BPC6 has been shown to participate in the regulation of *ABI4* (Mu et al., 2017),
410 and subcellular localization indicated that BPC6-GFP is in the nucleus of guard cells
411 (Figure 7A). To detect whether BPCs can directly regulate the expression of key
412 marker genes of stomatal development, we analyzed the transcript levels of both
413 *SCRM* and *SCRM2*, which can form a complex to regulate the functions of SPCH,
414 MUTE, and FAMA (Pillitteri and Torii, 2012). RT-PCR analysis indicated that the
415 expression levels of *SCRM* and *SCRM2* in the *bpc1 bpc2 bpc3 bpc4 bpc6 bpc7*
416 sextuple mutant are lower than in WT (Figure 7B). Further analysis showed that the
417 Stomatal Index (SI) was increased in the *bpc1 bpc2 bpc4 bpc6* quadruple mutant and
418 the *bpc1 bpc2 bpc3 bpc4 bpc6 bpc7* sextuple mutant, whereas the SI of BPC6-GFP
419 was decreased compared with WT (Figure 7C-E). These results suggest that BPCs can
420 mediate stomatal development by regulating the expression of *SCRM* and *SCRM2*.

421 **Developmental Pseudo-time Analysis of Marker Gene Expression**

422 To reconstruct the developmental trajectory during differentiation, we performed
423 pseudo-temporal ordering of cells (pseudo-time) from our scRNAseq data using
424 Monocle 2(Trapnell et al., 2014). In total, the pseudo-time path has three branches
425 (Figure 8A and B), and different cell clusters can be arranged relatively clearly at
426 different branch sites of the pseudo-time path (Figure 8B). In general, the different
427 developmental processes of stomatal lineage cells can be seen from PDC to GC
428 (Figure 8B). Surprisingly, PC was concentrated in a pseudo-time branch that was
429 significantly different from the other cell types (Figure 8B). Intriguingly, we found
430 that PDC and GMC could not be clearly distinguished on the pseudo-time curve
431 (Figure 8B). In principle, the distribution characteristics of different cell types on the
432 development trajectory can preliminarily determine the relationship between these
433 cells during the development period. The distribution of GMC and YGC in the
434 development trajectory is relatively concentrated, but MPC_2 and MPC_5 can be
435 found at several time points along the development trajectory, suggesting that the cell
436 development stage of MPC is more complex. Interestingly, we found that PDC and

437 EM show relatively similar distribution patterns in the development trajectory,
438 suggesting that their developmental stages are close. Although PC is mainly
439 distributed in branch 1 at the end stage of the development trajectory, it is also
440 distributed at other time points, which is consistent with the earlier development stage
441 of PC cells compared to stomatal cells. To investigate the pseudo-time patterns of
442 genes in each cluster, we performed heatmap analysis for all the highly expressed
443 genes (Figure 8C). In general, the pseudo-time patterns of all genes can be divided
444 into three clusters (Figure 8C). To analyze the pseudo-time patterns of representative
445 marker genes, we selected the top 5 marker genes in each cluster to analyze their
446 pseudo-time patterns (Figure 8D). As shown in Figure 8D, the heatmap of
447 pseudo-time of the top 5 marker genes shows that their pseudo-time pattern can be
448 classified into two clusters (Figure 8D). In the first cluster, the expression of all the
449 marker genes increases gradually along with the pseudo-time (Figure 8D). In contrast,
450 expression of marker genes in cluster 2 decreases at the end of the pseudo-time axis
451 (Figure 8D). In the first cluster, the marker genes are mainly from PC, suggesting that
452 PCs are at a more mature stage of development (Figure 8D). The second cluster can
453 be divided into three branches: in the first, expression of marker genes mainly from
454 GMC,YGC,GC and MPC first gradually increases to a maximum level, and then
455 decreases quickly along the pseudo-time; in the second branch, expression of marker
456 genes mainly from PDC and LM is very high at the beginning of development, but
457 quickly decreases along the pseudo-time; in the third branch, expression of the marker
458 genes mainly from MMC and EM is lower in all of the developmental periods along
459 the pseudo-time, and further declines at the last stage of pseudo-time (Figure 8D). It
460 can be seen from the heatmap and curves of pseudo-time that expression of *SPCH*,
461 *MUTE* and *FAMA* occurs mainly between PDC and MMC, MMC and M, and GMC
462 and GC (Figure 9A and B). Expression of the marker genes *EPF1*, *SPCH* and *MUTE*
463 is highly similar at the early stages of development (Figure 9A and B). As expected,
464 *EPF2*, *FAMA* and *SCRM* are mainly expressed in the EM and LM stages and exhibit a
465 similar pseudo-time pattern (Figure 9A and B). Although *SCRM* and *SCRM2* have

466 some functional interactions with *MUTE* and *SPCH* in the regulation of stomatal
467 lineage cell development, our pseudo-time results show that expression of the *SCRM*,
468 *SCRM2*, *MUTE* and *SPCH* genes is significantly different (Figure 9A and B).

469 **DISCUSSION**

470 Stomatal lineage cell fate decisions are traceable, irreversible, and produce
471 well-known differentiated cell types. We were able to investigate the interplay of
472 multiple fate-specific genetic programs and the effects of external environmental
473 factors on the fate decision of different cell types at the single cell level. A
474 combination of known marker genes and GO analysis enabled us to reliably classify
475 and define cell types (Figure 1, Figure S3). Transcripts of some marker genes (*SPCH*,
476 *MUTE* and *FAMA*) are enriched in specific types of stomatal lineage cells (Figure S3),
477 while those of other marker genes (*CRY1*, *PP2C*, *BCA4* and *CALS10*) are not (Figure
478 S3). Furthermore, a series of new marker genes were identified in different cell types
479 (Figure 2). We also analyzed the effects of some marker genes on stomatal lineage
480 cell development by checking the stomatal developmental patterns in the cotyledons
481 of the corresponding mutants (Figures 3, 6, and 7).

482 **Determination of cell types and marker genes**

483 The stomatal lineage cells can be classified into seven different types including PDC,
484 MMC, EM, LM, GMC, YGC and GC based on their developmental stages. To
485 determine the cell type we analyzed the feature plot of the selected marker genes in
486 specific cell types (Figure S3B). We used more than one marker genes for identifying
487 one cell type because marker genes are often expressed in more than one cell type and
488 to different levels (Figure 1). In the case of PDC, no known marker genes can be used,
489 but some marker genes are possibly expressed in PDC before entry into the stomatal
490 lineage cell pathway, such as *EFP2*, *TMM*, *BASL*, *SPCH* although their expression
491 levels are less than in MMC. The MMC, EM, LM, YGC and GC can be clearly
492 identified based on the existence of specific marker genes in each cluster. PC contains
493 chloroplasts and is difficult to distinguish from MPC (Figure 1C). Auxin is required
494 for the formation of the interdigitated cell pattern in leaf pavement cells through the
495 coordination of the two mutually exclusive ROP2 and ROP6 pathways (Xu et al.,
496 2011). The auxin-activated ROP2 pathway is essential for PIN1 polar localization at

497 the lobe apex by inhibiting its internalization (Xu et al., 2010). Therefore, we used
498 ROP2 and ROP6 as marker genes to identify PC. Based on these considerations we
499 propose that cluster 0 represents PC. We could not determine the cell type of cluster 9
500 with known marker genes (Figure 1C). Interestingly, we found that one marker gene,
501 *BAG6*, may be involved in regulating the biogenesis and distribution of stomata
502 (Figure S4). However, *bZIP6*, another marker gene of cluster 9, is specifically
503 expressed in the two pericycles in the phloem pole starting from the early root
504 elongation zone, suggesting that cluster 9 does not belong to epidermal cells. We
505 selected the top 10 marker genes in each cluster as representative marker genes for the
506 different cell types (Figure 2). Analysis of the marker genes in GC indicated that
507 some of them are involved in regulating the development and function of stomata
508 (Figure 2A), suggesting that the marker genes identified can be used for determining
509 the cell type.

510 **Potential factors that regulate the fate of stomatal lineage cells**

511 The stomatal lineage cell development is regulated by many important factors, such as
512 light, temperature, metabolism, and phytohormones (Pillitteri and Dong, 2013). In the
513 past, most studies using whole plant cells, could not clearly distinguish the special
514 functions of these factors in the different cell types. For instance, light- and
515 hormone-signaling can affect the entire process of stomatal lineage cell development
516 (Pillitteri and Dong, 2013). Based on scRNA-seq, combined with GO analysis, we
517 were able to identify the potential genes that regulate stomatal lineage cell
518 development. For example, GO heatmap analysis revealed that genes preferentially
519 expressed in YGC and GC are mainly involved in the response to oxidative stress,
520 abscisic acid, osmotic stress, and vacuolar activity (Figure 4). The GO heatmap
521 analysis also showed that GO terms enriched in MMC, EM, LM, and GMC are
522 relatively similar (Figure 4A), suggesting there are intense interactions in gene
523 expression and cell functions among these cells. GO terms enriched in LM and GMC
524 are involved in regulating the respiratory chain (Figure 4B), suggesting that the
525 differentiation from LM to GMC is an energy-intensive process. It should be noted
526 that genes highly expressed in MMC are involved in the response to bacterial

527 infection and in the MAPK signaling pathway (Figure 4B). Studies have shown that
528 bacterial infection can generate a systemic signal that is translocated from the mature
529 infected leaves to the developing leaves in the apical meristem, where it reduces
530 stomatal density by increasing epidermal cell expansion in the newly developing
531 leaves (Dutton et al., 2019). After infection fewer epidermal cells enter the stomatal
532 lineage during the early stages of leaf development (Dutton et al., 2019). Taken
533 together our results indicate that, genes expressed in MMC are required for
534 suppressing the biogenesis of stomatal cells in response to bacterial infection.
535 Interestingly, GO analysis revealed that genes expressed in PDCs and MMCs are
536 involved in the regulation of protein transport, vesicle-mediated transport and in
537 membrane protein complexes (Figure 4A).

538 Analysis of the new identified marker genes revealed that expression of *ATML1*
539 and *PDF1* was specifically enhanced in MMC. *ATML1* and *PDF1* show high
540 co-expression with *MUTE* and *SPCH* (Figure 2A and Figure S3A). Further analysis
541 revealed that *atml1-2* and *atml1-3* are deficient in the development of stomatal lineage
542 cells (Figure 3). In addition, the expression levels of both *SPCH* and *MUTE* were
543 decreased in *atml1-2* and *atml1-3*, compared with WT (Figure 3E). *ATML1* encodes a
544 homeobox protein similar to *GL2* and is expressed in both the apical and basal
545 daughter cells of the zygote as well as in its progeny (Peterson et al., 2013).
546 Expression of *ATML1* starts at the two-cell stage of embryo development and is later
547 restricted to the outermost epidermal cell layer (Iida et al., 2019). The *ATML1*
548 promoter is highly modular with each of its domains contributing to specific features
549 of the spatial and temporal expression of the gene (Takada et al., 2013). Double
550 mutant analysis with *pdf2*, another L1-specific gene, suggests that their functions are
551 partially redundant, since the loss of both genes results in abnormal shoot
552 development (Ogawa et al., 2015). Over-expression of *ATML1* can induce the
553 formation of stomata-like structures in the inner cells of the cotyledons in independent
554 lines (Peterson et al., 2013). Therefore, taken together, our results suggest that
555 *ATML1* can regulate the development of stomatal lineage cells by modulating the
556 expression of both *SPCH* and *MUTE*.

557 **Involvement of a TF regulatory network in regulating stomatal lineage cell**
558 **development**

559 It is well known that bHLH TFs play important roles in regulating stomatal lineage cell
560 cell development (MacAlister et al., 2007; Pillitteri et al., 2007). Recently, additional
561 new TFs that are involved in regulating the stomatal lineage cell development have
562 been identified, for example PIF4, MYB88, HDG2, GL2 (Casson et al., 2009;
563 Pillitteri and Dong, 2013). To identify new TFs that regulate stomatal lineage cell
564 development in special cell types, we analyzed potential TFs expressed in different
565 stomatal lineage cells. Analysis of the network of TFs indicated that PIF5, WRKY33,
566 BPC1, and BPC6 may act as the core TFs that regulate the differentiation from PDC
567 to GMC (Figure 5C and D). The BPC gene family has seven members in Arabidopsis
568 (Monfared et al., 2011). BPC belongs to GAGA binding proteins (GBPs), which bind
569 GA-rich elements (Biggin and Tjian, 1988; Kooiker et al., 2005; Monfared et al.,
570 2011). These GBPs are involved in regulating gene expression by interacting with
571 chromatin remodeling complexes like NURF and FACT (Lehmann, 2004). Expression
572 of *BPC* genes occurs widely, but to different extents, in various organs. These genes
573 play important roles in regulating the vegetative and reproductive development
574 (Kooiker et al., 2005; Monfared et al., 2011; Simonini et al., 2012; Simonini and
575 Kater, 2014; Mu et al., 2017; Shanks et al., 2018). Our results indicate that besides the
576 core TFs (e.g. SPCH, MUTE, FAMA, etc), a TF network comprising WRKY33,
577 BPC1/6, and PIF5 is required for modulating the development of stomatal cells.
578 Further analysis revealed that *wrky33* and the *bpc1 bpc2 bpc4 bpc6* quadruple mutant
579 are deficient in different stomatal lineage cells (Figure 6 and Figure 7). The
580 expression levels of *SCRM* and *SCRM2* in the *bpc1 bpc2 bpc3 bpc4 bpc6 bpc7*
581 sextuple mutant were less than in WT (Figure 7). These results suggest that WRKY33,
582 BPCs, and PIF5 act as the core TFs that regulate the differentiation from PDC to
583 GMC.

584 **The developmental trajectory of stomatal lineage cells**

585 To dissect the temporal and spatial distribution of stomatal lineage cells we performed
586 a pseudo-time analysis on scRNASeq data (Figure 8A and B). Pseudo-time patterns of
587 all genes can be divided into three clusters (Figure 8C). Further analysis of the top 5
588 selected marker genes in each cluster indicated that these marker genes can be
589 grouped into two clusters (Figure 8D). The first cluster mainly contains the markers
590 from MPC (Figure 8D). The second cluster can be divided into three sub-clusters: the
591 first sub-cluster includes the marker genes from GMC, YGC, GC and MPC; the
592 second sub-cluster contains the marker genes from PDC and LM; and the third
593 sub-cluster includes the marker genes from MMC and EM (Figure 8D). As typical
594 marker genes, *SPCH* and *MUTE* were found to be co-expressed with *EPF1*, *MKK5*
595 and *MKK9* (Figure 9A and B), suggesting that EPF1-MKK9/5 dependent signaling
596 can influence both the expression and the function of *SPCH* and *MUTE*. More
597 interestingly, light-signal receptor genes and stomatal lineage marker genes show
598 strong co-expression patterns (Figure 9A). In response to changes in light quality,
599 different light signal receptors rely on downstream COP1-YDA-MAPK signaling
600 pathways to regulate different stages of stomatal lineage development (Kang et al.,
601 2009). Our results show that *SCRM2* and *COP1* exhibit very similar pseudo-time
602 curves, while *SCRM* has the same pseudo-time curves as *PHYA* and *PHYB* (Figure 9A
603 and B). Unlike *PHYA* and *PHYB*, the pseudo-time curves of the blue receptor *CRY1* is
604 significantly different from those of *PHYA* and *PHYB* (Figure 9A and B). Surprisingly,
605 although *EPF1* and *EPF2* play very similar roles in regulating stomatal lineage cell
606 development, they exhibit distinct expression patterns (Figure 9A and B). It has been
607 reported that EPF2 activates ER signaling, leading to subsequent MAPK activation
608 and inhibition of stomatal lineage cell development, while EPFL9 prevents signal
609 transduction of MPK3 and MPK6 (Lee et al., 2015). In the pseudo-time course,
610 however, we observed that *MPK3* has the exact opposite expression pattern compared
611 with *EPF1* (Figure 9A and B).

612 The transition to GMC is coordinated through cell-cycle controls and is
613 promoted by MUTE (Han et al., 2018), while FAMA and FLP/MYB88 act in parallel

614 to antagonize GMC transition (Lai et al., 2005). The canonical G1 and
615 G1/S-regulating CYCD family member *CYCD5;1* is a MUTE target, implying that it
616 may promote symmetric cell division (SCD) commitment in a MUTE-dependent
617 manner (Han et al., 2018). Interestingly, *CYCD7;1* is not regulated by MUTE,
618 although *CYCD7;1* is specifically expressed in stomatal lineage cells (Adrian et al.,
619 2015). In addition to *CYCD5;1*, our results reveal that expression of *CYCA2;1* is
620 highly similar to that of *MUTE* and *SPCH* (Figures 9A and B). However, the
621 expression of *CYCA2;1* is restricted to the vascular tissues of leaves (Vanneste et al.,
622 2011). The co-expression of *MUTE* and *CYCA2;1* imply that the expression of these
623 two genes can be induced at a similar development time, but the expression of
624 *CYCA2;1* may not be regulated by MUTE.

625 **METHODS**

626 **Screening and Verification of Mutants**

627 T-DNA insertion mutants were obtained from the Arabidopsis Biological Resource
628 Center (ABRC) (Supplemental **Table 3**). Mutant lines homozygous for the T-DNA
629 insertion were identified by PCR analysis using gene-specific and T-DNA-specific
630 primers (Supplemental **Table 4**). In addition, we also generated the transgenic lines of
631 *BPC6-GFP*.

632 **Constructs for plant transformation**

633 To generate the pB7WGF2-*BPC6* constructs, the full-length cDNA of *BPC6* was
634 PCR-amplified using the primer pairs as described in Supplementary **Table 2**. Then
635 the PCR products were purified, and first cloned into pDNOR201 by BP Clonase
636 reactions (GATEWAY Cloning; Invitrogen) according to the manufacturer's
637 instructions to generate the pDNOR-*BPC6*. The resulting plasmids were recombined
638 into pB7WGF2 using LR Clonase reactions (GATEWAY Cloning; Invitrogen) to
639 generate the final constructs.

640 **PLANT TRANSFORMATION**

641 The pB7WGF2-*BPC6* constructs were transformed into *Agrobacterium tumefaciens*
642 strain GV3105 *via* electroporation. Then the *Agrobacterium tumefaciens* that
643 contained the constructs of pB7WGF2-*BPC6* was introduced into WT. The resulting
644 T1 transgenic plants of pB7WGF2-*BPC6* were selected by BASTA as described by
645 Sun et al (Sun et al., 2016). Homozygous transgenic plants were used in all
646 experiments.

647 **Cotyledon Collection and Protoplast Preparation**

648 We isolated protoplasts from cotyledons of five-day-old *Arabidopsis* seedlings as
649 described by Yoo, et al., (2007)(Yoo et al., 2007) with slight modifications to adjust
650 to the cotyledon tissue. Briefly, the cotyledons were harvested from seedlings
651 submerged in a solution (0.5 mM CaCl₂, 0.5 mM MgCl₂, 5 mM MES, 1.5% Cellulase
652 RS, 0.03% Pectolyase Y23, 0.25% BSA, actinomycin D [33 mg/L], and cordycepin
653 [100mg/L], pH 5.5) by vacuum infiltration for 10 min. The samples were then
654 incubated for 4 hours to isolate protoplasts. Afterwards, the isolated cells were
655 washed three times with 8% mannitol buffer to remove Mg²⁺. Cells were then filtered
656 with a 40 µm cell strainer. Cell activity was detected by trypan blue staining and cell
657 concentration was measured with a hemocytometer.

658 **Single-cell RNA-seq Library Preparation**

659 We prepared single-cell RNA-seq libraries with Chromium Single Cell 3' Gel
660 Beads-in-emulsion (GEM) Library & Gel Bead Kit v3 according to the user manual
661 supplied by the kit. In brief, GEMs were generated and barcoded, followed by post
662 GEM-RT cleanup and cDNA Amplification, and finally 3' Gene Expression Library
663 Construction. In the first step cells were diluted so that the majority (~90-99%) of
664 GEMs contained no cells, while the remainder mostly contained a single cell. The Gel
665 Beads were then dissolved, primers were released, and any co-partitioned cell was
666 lysed in order to generate full-length cDNA from poly-adenylated mRNA.
667 Subsequently, the first-strand cDNA from the post GEM-RT reaction mixture was
668 purified with SILANE magnetic beads. After purification, the barcoded full-length
669 cDNA was amplified via PCR to generate sufficient amounts for library construction.
670 In the third step, enzymatic fragmentation and size selection were used to optimize the

671 cDNA amplicon size. In addition, the TruSeq Read 1 (read 1 primer sequence) was
672 added to the molecules during GEM incubation. P5, P7, a sample index, and TruSeq
673 Read 2 (read 2 primer sequence) were added via End Repair. This was followed by
674 A-tailing, adaptor ligation, and PCR. The final libraries contained the P5 and P7
675 primers used in Illumina bridge amplification.

676 **Single-cell RNA-seq Data Preprocessing**

677 The Cell Ranger pipeline (version 3.0.0) provided by 10 \times Genomics was used to
678 demultiplex cellular barcodes and map reads to the TAIR10 reference genome.
679 Transcript quantifications were determined via the STAR aligner. We processed the
680 unique molecular identifier (UMI) count matrix using the R package Seurat (version
681 2.3.4). To remove low quality cells and likely multiple captures, we further applied
682 criteria to filter out cells with UMI/gene numbers outside the limit of the mean value
683 \pm 2 standard deviations, assuming a Gaussian distribution of each cell's UMI/gene
684 numbers. Following visual inspection of the distribution of cells by the fraction of
685 chloroplast genes expressed, we further discarded low-quality cells where $>40\%$ of
686 the counts belonged to chloroplast genes. After applying these quality control (QC)
687 criteria, 12,844 single cells and 32,833 genes in total remained and were included in
688 the downstream analyses. Library size normalization was performed in Seurat on the
689 filtered matrix to obtain normalized counts.

690 Genes with the highest variable expression amongst single cells were identified
691 using the method described in Macosko et al (Macosko et al., 2015). Briefly, the
692 average expression and dispersion were calculated for all genes, which were
693 subsequently placed into 11 bins based on expression. Principal component analysis
694 (PCA) was performed to reduce the dimensionality on the log transformed
695 gene-barcode matrices of the most variable genes. Cells were clustered via a
696 graph-based approach and visualized in 2-dimensions using tSNE. A likelihood ratio
697 test, which simultaneously tests for changes in mean expression and percentage of
698 cells expressing a gene, was used to identify significantly differentially expressed
699 genes (DEGs) between clusters. We also performed tSNE analyses and identified the
700 DEGs between clusters for the mesophyll and stomatal lineage cell populations.

701 Pseudotime trajectory analysis of single cell transcriptomes was conducted using
702 Monocle 2 (Trapnell et al., 2014). Genes with the most highly variable expression
703 were used for clustering the cells. Gene expression was then plotted as a function of
704 pseudo-time in Monocle 2 to track changes across pseudo-time. We also plotted TFs
705 and marker genes along the inferred developmental pseudo-time. The regulation
706 networks for the TFs and target genes were plotted by Cytoscape according to the
707 PlantTFDB database.

708 **Microscopy**

709 The cotyledons were observed 5 d after germination. The samples were harvested and
710 placed in 70% ethanol, cleared overnight at room temperature, and then stored in
711 Hoyer's Solution. Images of stomata were obtained from samples stored in Hoyer's
712 Solution and visualized using differential interference contrast microscopy with a
713 Leica DMi8 microscope. A Nikon D-ECLIPSE C1 laser confocal scanning
714 microscope was used for green fluorescent protein (GFP) fluorescence images.

715 **Gene Ontology (GO) Enrichment Analysis**

716 The enrichment of gene ontology (GO) terms and pathways for the DEGs were
717 analyzed using Metascape (<http://metascape.org/>) (Zhou et al., 2019).

718 **Accession Numbers**

719 Sequence data from this study can be found in the Arabidopsis Genome Initiative data
720 library under the following accession numbers: *WRKY33* (AT1G07890), *BPC1*
721 (AT2G01930), *BPC2* (AT1G14685), *BPC3* (AT1G68120), *BPC4* (AT2G21240),
722 *BPC6* (AT5G42520), *BPC7* (AT2G35550), *ATML1* (AT4G21750), *BAG6*
723 (AT2G46240), *bZIP6* (AT2G22850). Single cell RNA sequence data are available at
724 the <https://dataview.ncbi.nlm.nih.gov/?search=SUB6947465>
725 (<https://www.ncbi.nlm.nih.gov>) .

726 **ACKNOWLEDGEMENTS**

727 We are grateful to ABRC for the Arabidopsis seeds. This research was supported by
728 the National Natural Science Foundation of China (31670233) and the Program of

729 Introducing Talents of Discipline to Universities. We thank Prof. Charles Gasser for
730 providing the *bpc double, triple, quadruple, and sextuple* mutant seeds.

731 **AUTHOR CONTRIBUTIONS**

732 XS designed the study; ZL, YZ, JG, ZZ, JL, ZT, JW, RW, BZ, WL, TL, YH and YH
733 performed the research; RJ, YM and XS analyzed the data; XS and RJ wrote the paper.
734 All authors discussed the results and made comments on the manuscript.

735 **DECLARATION OF INTERESTS**

736 The authors declare that they have no conflict of interest.

737 **REFERENCES**

738 **Adrian, J., Chang, J., Ballenger, C.E., Bargmann, B.O.R., Alassimone, J., Davies,
739 K.A., Lau, O.S., Matos, J.L., Hachez, C., Lanctot, A., Vaten, A.,
740 Birnbaum, K.D., and Bergmann, D.C.** (2015). Transcriptome Dynamics of
741 the Stomatal Lineage: Birth, Amplification, and Termination of a
742 Self-Renewing Population. *Developmental Cell* **33**, 107-118.

743 **Amsbury, S., Hunt, L., Elhaddad, N., Baillie, A., Lundgren, M., Verhertbruggen,
744 Y., Scheller, H.V., Knox, J.P., Fleming, A.J., and Gray, J.E.** (2016).
745 Stomatal Function Requires Pectin De-methyl-esterification of the Guard Cell
746 Wall. *Current Biology* **26**, 2899-2906.

747 **Barton, K.A., Schattat, M.H., Jakob, T., Hause, G., Wilhelm, C., McKenna, J.F.,
748 Mathe, C., Runions, J., Van Damme, D., and Mathur, J.** (2016). Epidermal
749 Pavement Cells of *Arabidopsis* Have Chloroplasts. *Plant Physiol* **171**,
750 723-726.

751 **Bergmann, D.C., and Sack, F.D.** (2007). Stomatal development. *Annu Rev Plant
752 Biol* **58**, 163-181.

753 **Bergmann, D.C., Lukowitz, W., and Somerville, C.R.** (2004). Stomatal
754 development and pattern controlled by a MAPKK kinase. *Science* **304**,
755 1494-1497.

756 **Biggin, M.D., and Tjian, R.** (1988). Transcription factors that activate the

757 Ultrabithorax promoter in developmentally staged extracts. *Cell* **53**, 699-711.

758 **Casson, S.A., Franklin, K.A., Gray, J.E., Grierson, C.S., Whitelam, G.C., and**
759 **Hetherington, A.M.** (2009). phytochrome B and PIF4 Regulate Stomatal
760 Development in Response to Light Quantity. *Current Biology* **19**, 229-234.

761 **Chanroj, S., Padmanaban, S., Czerny, D.D., Jauh, G.Y., and Sze, H.** (2013). K⁺
762 transporter AtCHX17 with its hydrophilic C tail localizes to membranes of the
763 secretory/endocytic system: role in reproduction and seed set. *Mol Plant* **6**,
764 1226-1246.

765 **Chen, L., Guan, L.P., Qian, P.P., Xu, F., Wu, Z.L., Wu, Y.J., He, K., Gou, X.P.,**
766 **Li, J., and Hou, S.W.** (2016). NRPB3, the third largest subunit of RNA
767 polymerase II, is essential for stomatal patterning and differentiation in
768 *Arabidopsis*. *Development* **143**, 1600-1611.

769 **Dong, J., MacAlister, C.A., and Bergmann, D.C.** (2009). BASL controls
770 asymmetric cell division in *Arabidopsis*. *Cell* **137**, 1320-1330.

771 **Dutton, C., Horak, H., Hepworth, C., Mitchell, A., Ton, J., Hunt, L., and Gray,**
772 **J.E.** (2019). Bacterial infection systemically suppresses stomatal density. *Plant*
773 *Cell Environ* **42**, 2411-2421.

774 **Engineer, C.B., Ghassemian, M., Anderson, J.C., Peck, S.C., Hu, H.H., and**
775 **Schroeder, J.I.** (2015). Carbonic anhydrases, EPF2 and a novel protease
776 mediate CO₂ control of stomatal development (vol 513, pg 246, 2014). *Nature*
777 **526**, 458-458.

778 **Fu, C., Hou, Y., Ge, J., Zhang, L., Liu, X., Huo, P., and Liu, J.** (2019). Increased
779 fes1a thermotolerance is induced by BAG6 knockout. *Plant Mol Biol* **100**,
780 73-82.

781 **Fu, Y., Gu, Y., Zheng, Z., Wasteneys, G., and Yang, Z.** (2005). *Arabidopsis*
782 interdigitating cell growth requires two antagonistic pathways with opposing
783 action on cell morphogenesis. *Cell* **120**, 687-700.

784 **Geisler, M., Nadeau, J., and Sack, F.D.** (2000). Oriented asymmetric divisions that
785 generate the stomatal spacing pattern in *Arabidopsis* are disrupted by the too

786 many mouths mutation. *Plant Cell* **12**, 2075-2086.

787 **Gray, J.** (2005). Guard cells: transcription factors regulate stomatal movements. *Curr*
788 *Biol* **15**, R593-595.

789 **Han, S.K., and Torii, K.U.** (2016). Lineage-specific stem cells, signals and
790 asymmetries during stomatal development. *Development* **143**, 1259-1270.

791 **Han, S.K., Qi, X., Sugihara, K., Dang, J.H., Endo, T.A., Miller, K.L., Kim, E.D.,**
792 **Miura, T., and Torii, K.U.** (2018). MUTE Directly Orchestrates Cell-State
793 Switch and the Single Symmetric Division to Create Stomata. *Dev Cell* **45**,
794 303-315 e305.

795 **Hara, K., Kajita, R., Torii, K.U., Bergmann, D.C., and Kakimoto, T.** (2007). The
796 secretory peptide gene EPF1 enforces the stomatal one-cell-spacing rule. *Gene*
797 *Dev* **21**, 1720-1725.

798 **Hronkova, M., Wiesnerova, D., Simkova, M., Skupa, P., Dewitte, W., Vrablova,**
799 **M., Zazimalova, E., and Santrucek, J.** (2015). Light-induced
800 STOMAGEN-mediated stomatal development in *Arabidopsis* leaves. *Journal*
801 of Experimental Botany **66**, 4621-4630.

802 **Huang, S., Waadt, R., Nuhkat, M., Kollist, H., Hedrich, R., and Roelfsema,**
803 **M.R.G.** (2019). Ca(2+) signals in guard cells enhance the efficiency by which
804 ABA triggers stomatal closure. *New Phytol.*

805 **Hunt, L., and Gray, J.E.** (2009a). The signaling peptide EPF2 controls asymmetric
806 cell divisions during stomatal development. *Curr Biol* **19**, 864-869.

807 **Hunt, L., and Gray, J.E.** (2009b). The Signaling Peptide EPF2 Controls Asymmetric
808 Cell Divisions during Stomatal Development. *Current Biology* **19**, 864-869.

809 **Iida, H., Yoshida, A., and Takada, S.** (2019). ATML1 activity is restricted to the
810 outermost cells of the embryo through post-transcriptional repressions.
811 *Development* **146**.

812 **Kabbage, M., and Dickman, M.B.** (2008). The BAG proteins: a ubiquitous family of
813 chaperone regulators. *Cell Mol Life Sci* **65**, 1390-1402.

814 **Kanaoka, M.M., Pillitteri, L.J., Fujii, H., Yoshida, Y., Bogenschutz, N.L.,**

815 **Takabayashi, J., Zhu, J.K., and Torii, K.U.** (2008). SCREAM/ICE1 and
816 SCREAM2 specify three cell-state transitional steps leading to *Arabidopsis*
817 stomatal differentiation. *Plant Cell* **20**, 1775-1785.

818 **Kang, C.Y., Lian, H.L., Wang, F.F., Huang, J.R., and Yang, H.Q.** (2009).
819 Cryptochromes, Phytochromes, and COP1 Regulate Light-Controlled
820 Stomatal Development in *Arabidopsis*. *Plant Cell* **21**, 2624-2641.

821 **Kim, T.W., Michniewicz, M., Bergmann, D.C., and Wang, Z.Y.** (2012).
822 Brassinosteroid regulates stomatal development by GSK3-mediated inhibition
823 of a MAPK pathway. *Nature* **482**, 419-U1526.

824 **Kooiker, M., Airoldi, C.A., Losa, A., Manzotti, P.S., Finzi, L., Kater, M.M., and**
825 **Colombo, L.** (2005). BASIC PENTACYSTEINE1, a GA binding protein that
826 induces conformational changes in the regulatory region of the homeotic
827 *Arabidopsis* gene SEEDSTICK. *Plant Cell* **17**, 722-729.

828 **Lai, L.B., Nadeau, J.A., Lucas, J., Lee, E.K., Nakagawa, T., Zhao, L.M., Geisler,**
829 **M., and Sack, F.D.** (2005). The *Arabidopsis* R2R3 MYB proteins FOUR
830 LIPS and MYB88 restrict divisions late in the stomatal cell lineage. *Plant Cell*
831 **17**, 2754-2767.

832 **Lampard, G.R., MacAlister, C.A., and Bergmann, D.C.** (2008). *Arabidopsis*
833 Stomatal Initiation Is Controlled by MAPK-Mediated Regulation of the bHLH
834 SPEECHLESS. *Science* **322**, 1113-1116.

835 **Lampard, G.R., Lukowitz, W., Ellis, B.E., and Bergmann, D.C.** (2009). Novel and
836 Expanded Roles for MAPK Signaling in *Arabidopsis* Stomatal Cell Fate
837 Revealed by Cell Type-Specific Manipulations. *Plant Cell* **21**, 3506-3517.

838 **Lawson, T.** (2009). Guard cell photosynthesis and stomatal function. *New Phytol* **181**,
839 13-34.

840 **Lee, J.S., Hnilova, M., Maes, M., Lin, Y.C.L., Putarjunan, A., Han, S.K., Avila,**
841 **J., and Torii, K.U.** (2015). Competitive binding of antagonistic peptides
842 fine-tunes stomatal patterning. *Nature* **522**, 435-+.

843 **Lee, J.S., Kuroha, T., Hnilova, M., Khatayevich, D., Kanaoka, M.M., McAbee,**

844 **J.M., Sarikaya, M., Tamerler, C., and Torii, K.U.** (2012). Direct interaction
845 of ligand-receptor pairs specifying stomatal patterning. *Gene Dev* **26**, 126-136.

846 **Lee, J.Y., Colinas, J., Wang, J.Y., Mace, D., Ohler, U., and Benfey, P.N.** (2006).
847 Transcriptional and posttranscriptional regulation of transcription factor
848 expression in *Arabidopsis* roots. *Proc Natl Acad Sci U S A* **103**, 6055-6060.

849 **Lehmann, M.** (2004). Anything else but GAGA: a nonhistone protein complex
850 reshapes chromatin structure. *Trends in genetics : TIG* **20**, 15-22.

851 **Li, J., Brader, G., and Palva, E.T.** (2008). Kunitz trypsin inhibitor: an antagonist of
852 cell death triggered by phytopathogens and fumonisin b1 in *Arabidopsis*. *Mol*
853 *Plant* **1**, 482-495.

854 **Li, Y., Kabbage, M., Liu, W., and Dickman, M.B.** (2016). Aspartyl
855 Protease-Mediated Cleavage of BAG6 Is Necessary for Autophagy and Fungal
856 Resistance in Plants. *Plant Cell* **28**, 233-247.

857 **Liang, H., Zhang, Y., Martinez, P., Rasmussen, C.G., Xu, T., and Yang, Z.** (2018).
858 The Microtubule-Associated Protein IQ67 DOMAIN5 Modulates Microtubule
859 Dynamics and Pavement Cell Shape. *Plant Physiol* **177**, 1555-1568.

860 **MacAlister, C.A., Ohashi-Ito, K., and Bergmann, D.C.** (2007). Transcription factor
861 control of asymmetric cell divisions that establish the stomatal lineage. *Nature*
862 **445**, 537-540.

863 **Macosko, E.Z., Basu, A., Satija, R., Nemesh, J., Shekhar, K., Goldman, M.,**
864 **Tirosh, I., Bialas, A.R., Kamitaki, N., Martersteck, E.M., Trombetta, J.J.,**
865 **Weitz, D.A., Sanes, J.R., Shalek, A.K., Regev, A., and McCarroll, S.A.**
866 (2015). Highly Parallel Genome-wide Expression Profiling of Individual Cells
867 Using Nanoliter Droplets. *Cell* **161**, 1202-1214.

868 **Maresova, L., and Sychrova, H.** (2006). *Arabidopsis thaliana* CHX17 gene
869 complements the *kha1* deletion phenotypes in *Saccharomyces cerevisiae*.
870 *Yeast* **23**, 1167-1171.

871 **Melotto, M., Underwood, W., Koczan, J., Nomura, K., and He, S.Y.** (2006). Plant
872 stomata function in innate immunity against bacterial invasion. *Cell* **126**,

873 969-980.

874 **Monfared, M.M., Simon, M.K., Meister, R.J., Roig-Villanova, I., Kooiker, M.,**
875 **Colombo, L., Fletcher, J.C., and Gasser, C.S.** (2011). Overlapping and
876 antagonistic activities of BASIC PENTACYSTEINE genes affect a range of
877 developmental processes in *Arabidopsis*. *Plant J* **66**, 1020-1031.

878 **Mu, Y., Zou, M., Sun, X., He, B., Xu, X., Liu, Y., Zhang, L., and Chi, W.** (2017).
879 BASIC PENTACYSTEINE Proteins Repress ABSCISIC ACID
880 INSENSITIVE4 Expression via Direct Recruitment of the
881 Polycomb-Repressive Complex 2 in *Arabidopsis* Root Development. *Plant*
882 *Cell Physiol* **58**, 607-621.

883 **Mucha, S., Heinzlmeir, S., Kriechbaumer, V., Strickland, B., Kirchhelle, C.,**
884 **Choudhary, M., Kowalski, N., Eichmann, R., Huckelhoven, R., Grill, E.,**
885 **Kuster, B., and Glawischnig, E.** (2019). The Formation of a Camalexin
886 Biosynthetic Metabolon. *Plant Cell* **31**, 2697-2710.

887 **Muller, T.M., Bottcher, C., Morbitzer, R., Gotz, C.C., Lehmann, J., Lahaye, T.,**
888 **and Glawischnig, E.** (2015). TRANSCRIPTION ACTIVATOR-LIKE
889 EFFECTOR NUCLEASE-Mediated Generation and Metabolic Analysis of
890 Camalexin-Deficient *cyp71a12 cyp71a13* Double Knockout Lines. *Plant*
891 *Physiol* **168**, 849-858.

892 **Nadeau, J.A., and Sack, F.D.** (2002). Control of stomatal distribution on the
893 *Arabidopsis* leaf surface. *Science* **296**, 1697-1700.

894 **Nafisi, M., Goregaoker, S., Botanga, C.J., Glawischnig, E., Olsen, C.E., Halkier,**
895 **B.A., and Glazebrook, J.** (2007). *Arabidopsis* cytochrome P450
896 monooxygenase 71A13 catalyzes the conversion of indole-3-acetaldoxime in
897 camalexin synthesis. *Plant Cell* **19**, 2039-2052.

898 **Niu, M.L., Huang, Y., Sun, S.T., Sun, J.Y., Cao, H.S., Shabala, S., and Bie, Z.L.**
899 (2018). Root respiratory burst oxidase homologue-dependent H₂O₂
900 production confers salt tolerance on a grafted cucumber by controlling Na⁺
901 exclusion and stomatal closure. *Journal of Experimental Botany* **69**,

902 3465-3476.

903 **Ogawa, E., Yamada, Y., Sezaki, N., Kosaka, S., Kondo, H., Kamata, N., Abe, M.,**
904 **Komeda, Y., and Takahashi, T.** (2015). ATML1 and PDF2 Play a
905 Redundant and Essential Role in *Arabidopsis* Embryo Development. *Plant*
906 *Cell Physiol* **56**, 1183-1192.

907 **Ohashi-Ito, K., and Bergmann, D.C.** (2006). *Arabidopsis* FAMA controls the final
908 proliferation/differentiation switch during stomatal development. *Plant Cell* **18**,
909 2493-2505.

910 **Peterson, K.M., Shyu, C., Burr, C.A., Horst, R.J., Kanaoka, M.M., Omae, M.,**
911 **Sato, Y., and Torii, K.U.** (2013). *Arabidopsis* homeodomain-leucine zipper
912 IV proteins promote stomatal development and ectopically induce stomata
913 beyond the epidermis. *Development* **140**, 1924-1935.

914 **Pillitteri, L.J., and Torii, K.U.** (2012). Mechanisms of Stomatal Development. *Annu*
915 *Rev Plant Biol* **63**, 591-614.

916 **Pillitteri, L.J., and Dong, J.** (2013). Stomatal development in *Arabidopsis*.
917 *Arabidopsis Book* **11**, e0162.

918 **Pillitteri, L.J., Sloan, D.B., Bogenschutz, N.L., and Torii, K.U.** (2007).
919 Termination of asymmetric cell division and differentiation of stomata. *Nature*
920 **445**, 501-505.

921 **Pilot, G., Lacombe, B., Gaymard, F., Cherel, I., Boucherez, J., Thibaud, J.B., and**
922 **Sentenac, H.** (2001). Guard cell inward K⁺ channel activity in *arabidopsis*
923 involves expression of the twin channel subunits KAT1 and KAT2. *J Biol*
924 *Chem* **276**, 3215-3221.

925 **Pitzschke, A., Xue, H., Persak, H., Datta, S., and Seifert, G.J.** (2016).
926 Post-Translational Modification and Secretion of Azelaic Acid Induced 1
927 (AZI1), a Hybrid Proline-Rich Protein from *Arabidopsis*. *Int J Mol Sci* **17**.

928 **Rajniak, J., Barco, B., Clay, N.K., and Sattely, E.S.** (2015). A new cyanogenic
929 metabolite in *Arabidopsis* required for inducible pathogen defence. *Nature* **525**,
930 376-379.

931 **Rudall, P.J., Hilton, J., and Bateman, R.M.** (2013). Several developmental and
932 morphogenetic factors govern the evolution of stomatal patterning in land
933 plants. *New Phytologist* **200**, 598-614.

934 **Shanks, C.M., Hecker, A., Cheng, C.Y., Brand, L., Collani, S., Schmid, M.,**
935 **Schaller, G.E., Wanke, D., Harter, K., and Kieber, J.J.** (2018). Role of
936 BASIC PENTACYSTEINE transcription factors in a subset of cytokinin
937 signaling responses. *Plant J* **95**, 458-473.

938 **Shpak, E.D., McAbee, J.M., Pillitteri, L.J., and Torii, K.U.** (2005). Stomatal
939 patterning and differentiation by synergistic interactions of receptor kinases.
940 *Science* **309**, 290-293.

941 **Simonini, S., and Kater, M.M.** (2014). Class I BASIC PENTACYSTEINE factors
942 regulate HOMEOBOX genes involved in meristem size maintenance. *J Exp*
943 *Bot* **65**, 1455-1465.

944 **Simonini, S., Roig-Villanova, I., Gregis, V., Colombo, B., Colombo, L., and Kater,**
945 **M.M.** (2012). Basic pentacysteine proteins mediate MADS domain complex
946 binding to the DNA for tissue-specific expression of target genes in
947 *Arabidopsis*. *Plant Cell* **24**, 4163-4172.

948 **Song, Y., Miao, Y., and Song, C.P.** (2014). Behind the scenes: the roles of reactive
949 oxygen species in guard cells. *New Phytol* **201**, 1121-1140.

950 **Sugano, S.S., Shimada, T., Imai, Y., Okawa, K., Tamai, A., Mori, M., and**
951 **Hara-Nishimura, I.** (2010). Stomagen positively regulates stomatal density in
952 *Arabidopsis*. *Nature* **463**, 241-U130.

953 **Sun, X., Xu, D., Liu, Z., Kleine, T., and Leister, D.** (2016). Functional relationship
954 between mTERF4 and GUN1 in retrograde signaling. *J Exp Bot* **67**,
955 3909-3924.

956 **Szyroki, A., Ivashikina, N., Dietrich, P., Roelfsema, M.R.G., Ache, P., Reintanz,**
957 **B., Deeken, R., Godde, M., Felle, H., Steinmeyer, R., Palme, K., and**
958 **Hedrich, R.** (2001). KAT1 is not essential for stomatal opening. *P Natl Acad*
959 *Sci USA* **98**, 2917-2921.

960 **Takada, S., Takada, N., and Yoshida, A.** (2013). ATML1 promotes epidermal cell
961 differentiation in *Arabidopsis* shoots. *Development* **140**, 1919-1923.

962 **Trapnell, C., Cacchiarelli, D., Grimsby, J., Pokharel, P., Li, S., Morse, M.,**
963 **Lennon, N.J., Livak, K.J., Mikkelsen, T.S., and Rinn, J.L.** (2014). The
964 dynamics and regulators of cell fate decisions are revealed by pseudotemporal
965 ordering of single cells. *Nat Biotechnol* **32**, 381-386.

966 **Underwood, W., Melotto, M., and He, S.Y.** (2007). Role of plant stomata in
967 bacterial invasion. *Cell Microbiol* **9**, 1621-1629.

968 **Vanneste, S., Coppens, F., Lee, E., Donner, T.J., Xie, Z., Van Isterdael, G.,**
969 **Dhondt, S., De Winter, F., De Rybel, B., Vuylsteke, M., De Veylder, L.,**
970 **Friml, J., Inze, D., Grotewold, E., Scarpella, E., Sack, F., Beemster, G.T.,**
971 **and Beeckman, T.** (2011). Developmental regulation of CYCA2s contributes
972 to tissue-specific proliferation in *Arabidopsis*. *EMBO J* **30**, 3430-3441.

973 **von Groll, U., and Altmann, T.** (2001). Stomatal cell biology. *Current Opinion in*
974 *Plant Biology* **4**, 555-560.

975 **Xu, T., Nagawa, S., and Yang, Z.** (2011). Uniform auxin triggers the Rho
976 GTPase-dependent formation of interdigitation patterns in pavement cells.
977 *Small GTPases* **2**, 227-232.

978 **Xu, T., Wen, M., Nagawa, S., Fu, Y., Chen, J.G., Wu, M.J., Perrot-Rechenmann,**
979 **C., Friml, J., Jones, A.M., and Yang, Z.** (2010). Cell surface- and rho
980 GTPase-based auxin signaling controls cellular interdigitation in *Arabidopsis*.
981 *Cell* **143**, 99-110.

982 **Yoo, S.D., Cho, Y.H., and Sheen, J.** (2007). *Arabidopsis* mesophyll protoplasts: a
983 versatile cell system for transient gene expression analysis. *Nat Protoc* **2**,
984 1565-1572.

985 **Zeng, W., Melotto, M., and He, S.Y.** (2010). Plant stomata: a checkpoint of host
986 immunity and pathogen virulence. *Curr Opin Biotechnol* **21**, 599-603.

987 **Zhang, C., Mallory, E.L., and Szymanski, D.B.** (2013). ARP2/3 localization in
988 *Arabidopsis* leaf pavement cells: a diversity of intracellular pools and

989 cytoskeletal interactions. *Front Plant Sci* **4**, 238.

990 **Zhang, D., Tian, C., Yin, K., Wang, W., and Qiu, J.L.** (2019). Postinvasive
991 Bacterial Resistance Conferred by Open Stomata in Rice. *Mol Plant Microbe*
992 *Interact* **32**, 255-266.

993 **Zhang, J.Y., He, S.B., Li, L., and Yang, H.Q.** (2014). Auxin inhibits stomatal
994 development through MONOPTEROS repression of a mobile peptide gene
995 STOMAGEN in mesophyll. *P Natl Acad Sci USA* **111**, E3015-E3023.

996 **Zhou, Y., Zhou, B., Pache, L., Chang, M., Khodabakhshi, A.H., Tanaseichuk, O.,**
997 **Benner, C., and Chanda, S.K.** (2019). Metascape provides a
998 biologist-oriented resource for the analysis of systems-level datasets. *Nat*
999 *Commun* **10**, 1523.

1000

1001 **FIGURE LEGENDS**

1002 Figure 1. Identification of the cell types with representative marker genes. **(A)**
1003 Scheme of expression of marker genes in different cell types. **(B)** Analysis of the
1004 dynamic pattern of marker genes during development of stomata. **(C)** Identification of
1005 the cell types according to the expression pattern of markers in each cell cluster.

1006 Figure 2. Identification of novel marker genes for each cluster. **(A)** Heatmap of
1007 expression of representative marker genes in each cluster. **(B)** Violin_plots show
1008 expression of representative marker genes in each of cell types. PDC: protodermal
1009 cells, PC: pavement cell, M: meristemoid, GMC: guard mother cell, GC: guard cell,
1010 MMC: meristemoid mother cell, EM: early stage meristemoid, LM: late stage
1011 meristemoid, YGC: young guard cell, MPC: mesophyll cell, u.k.: unknown.

1012 Figure 3. ATML1 is involved in regulating the development of stomata. **(A-D)**
1013 Analysis of stomatal development of 5-day-old seedlings of *atml1-2* (in Ler
1014 background), *atml1-3* (in Col background), Ler and Col are used as controls. **(E-F)**
1015 Quantitative analysis of **A-D**. **(G)** qPCR analysis of the expression of *SPCH* and
1016 *MUTE* in 5-day-old seedlings of *atml1-2*, *atml1-3*, Ler and Col. Error bars represent

1017 standard errors (S.E.). *: p<0.05, **: p<0.01, one-way ANOVA analysis versus Col.
1018 Scale bar: 50 μ m in **A-D**.

1019 Figure 4. GO analysis of the genes that expressed in different cell types. **(A)**
1020 GO-heatmap analysis of the genes with the highest variable expression in different
1021 clusters. **(B)** Same analysis as in A for MMC, GMC, EM and LM.

1022 Figure 5. Identification of regulatory networks of transcription factors in different cell
1023 types. **(A)** Identification of the transcription factors in different cell types. **(B)**
1024 Analysis of the regulatory network of transcription factors in MPC and PC. **(C)**
1025 Analysis of the regulatory network of transcription factors in PC and GC. **(D)**
1026 Analysis of the regulatory network of transcription factors in MMC, EM, LM and
1027 GMC. **(E)** Analysis of the regulatory network of transcription factors in PDC and
1028 GMC.

1029 Figure 6. Analysis of feature plots and function of core TFs. **(A)** Feature plots of the
1030 expression of representative TFs in different clusters. **(B)** Developmental pattern of
1031 stomatal lineage cells of cotyledons of five-day-old seedlings of *wrky33*, with wild
1032 type (WT) used as control. **(C)** Frequency of cell types calculated from **(B)**. Error bars
1033 represent standard errors (S.E.). *: p<0.05, **: p<0.01, one-way ANOVA analysis
1034 versus WT. Scale bar: 50 μ m in **B**.

1035 Figure 7. BPC proteins are involved in regulating the development of stomata. **(A)**
1036 Analysis of the subcellular localization of BPC6-GFP. **(B)** qPCR analysis of the
1037 expression of *SCRM* and *SCRM2* in the *bpc* sextuple mutant. **(C)** Developmental
1038 patterns of stomatal lineage cells in cotyledons of 5-day-old seedlings of *bpc* mutants
1039 and transgenic plants, WT was use as control. **(D)** Frequency of cell types calculated
1040 from **(C)**. **(E)** Number of epidermal cells of mutants grown on MS medium. Error
1041 bars represent standard errors (S.E.). *: p<0.05, **: p<0.01, one-way
1042 ANOVA analysis versus WT. Scale bar: 50 μ m in **A** and **C**.

1043 Figure 8. Pseudotime analysis of clusters and the selected marker genes. **(A)**
1044 Distribution of cells of each cluster on the pseudotime trajectory. **(B)** Pseudotime
1045 trajectory of single-cell transcriptomics data colored according to the cluster labels.

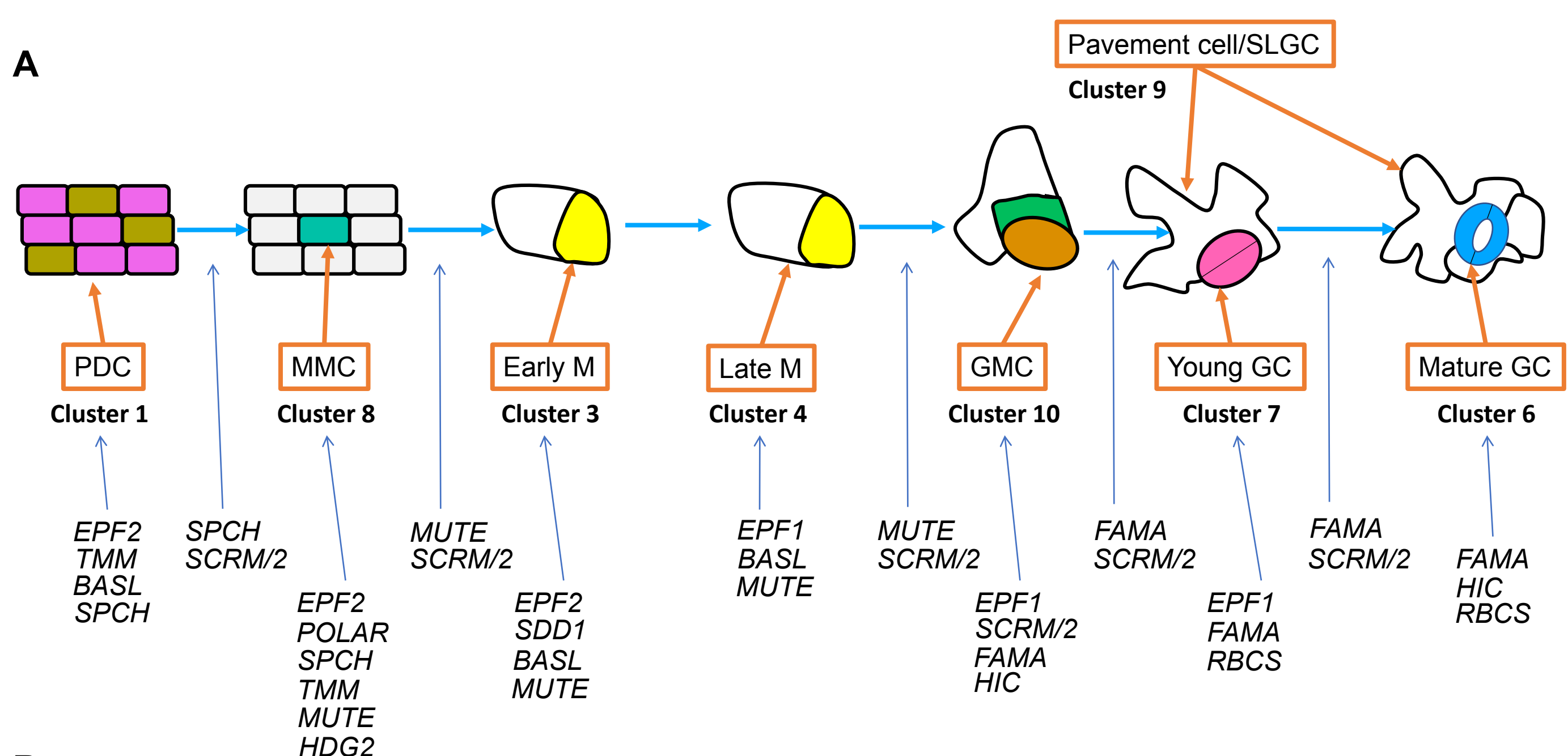
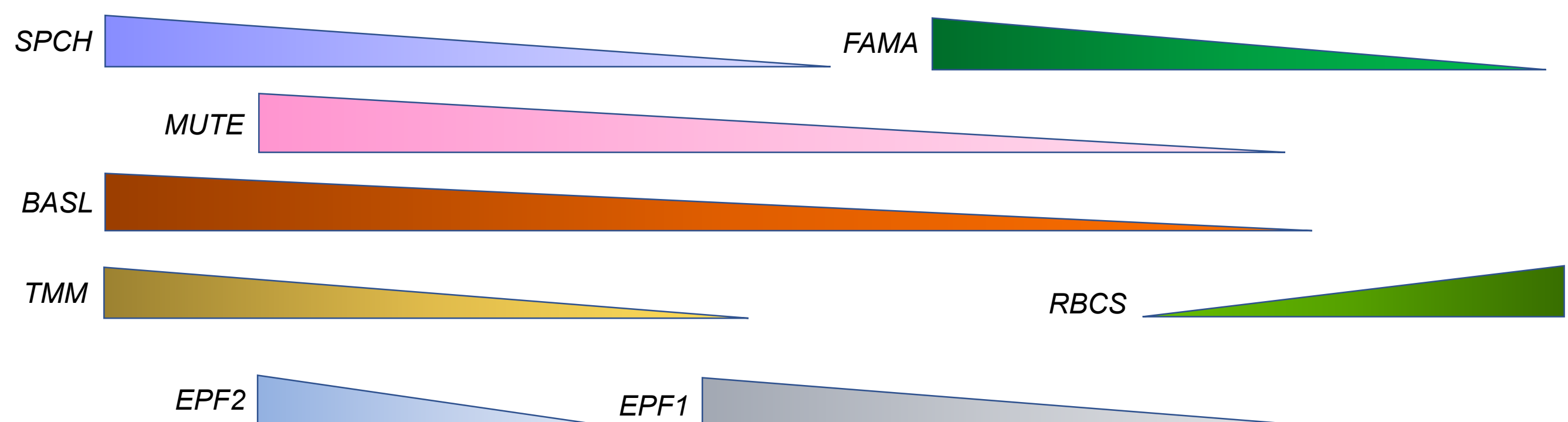
1046 Most cells were distributed along main stem, although two small branches were
1047 detected near the main path. **(C)** Clustering of all genes during pseudotime
1048 progression. **(D)** Clustering and expression kinetics of representative genes along
1049 pseudotime progression of stomatal lineage cells.

1050 Figure 9. Pseudo-time analysis of known marker genes. **(A)** Clustering of
1051 representative genes along pseudo-time progression of stomatal lineage cells. **(B)**
1052 Gene expression kinetics along pseudo-time progression of representative genes.

1053

1054

1055

A**B****C**

bioRxiv preprint doi: <https://doi.org/10.1101/2020.02.13.947549>; this version posted February 14, 2020. The copyright holder for this preprint (which was not certified by peer review) is the author/funder, who has granted bioRxiv a license to display the preprint in perpetuity. It is made available under aCC-BY-NC-ND 4.0 International license.

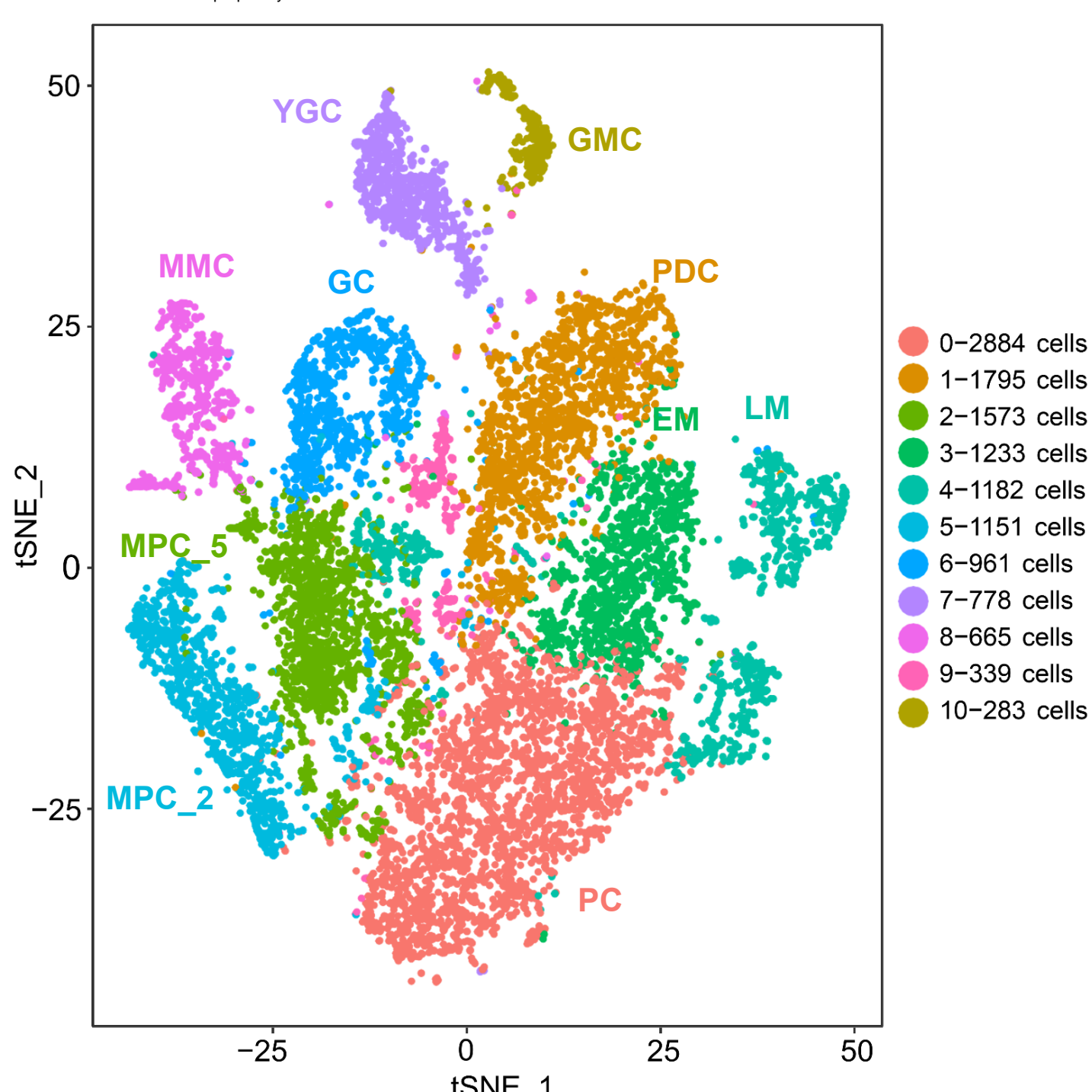


Figure 1. Identification of the cell types with representative marker genes. **(A)** Scheme of expression of marker genes in different cell types. **(B)** Analysis of the dynamic pattern of marker genes during development of stomata. **(C)** Identification of the cell types according to the expression pattern of markers in each cell cluster.

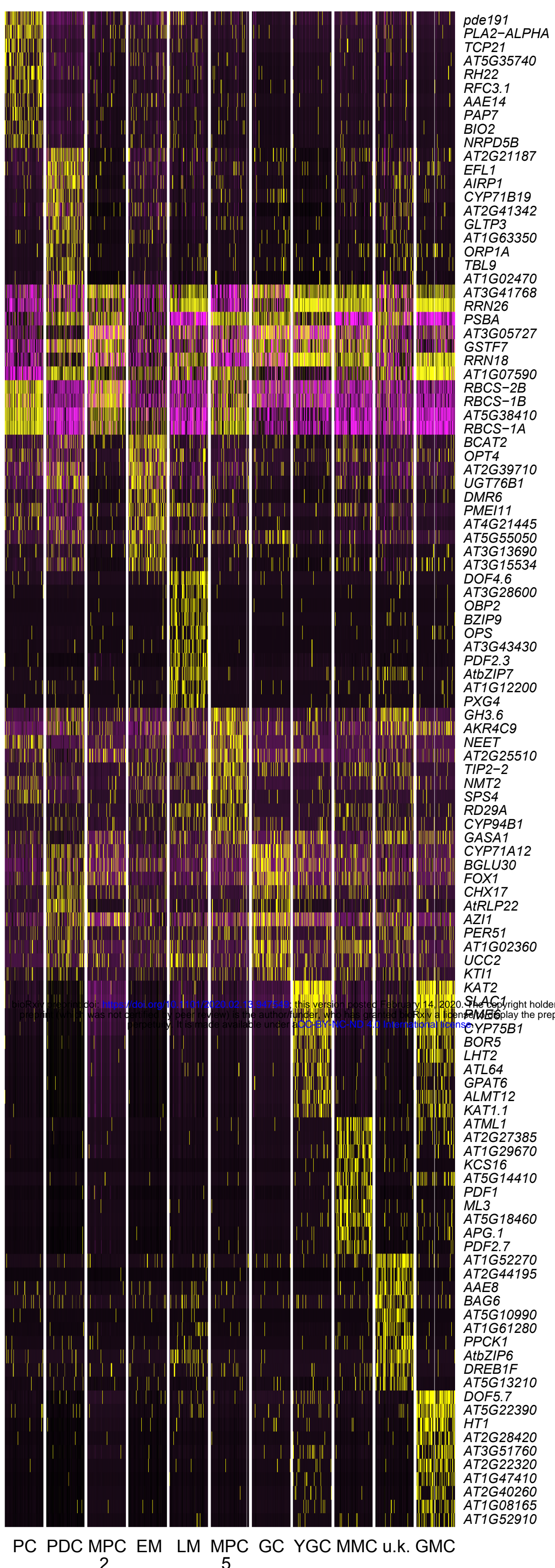
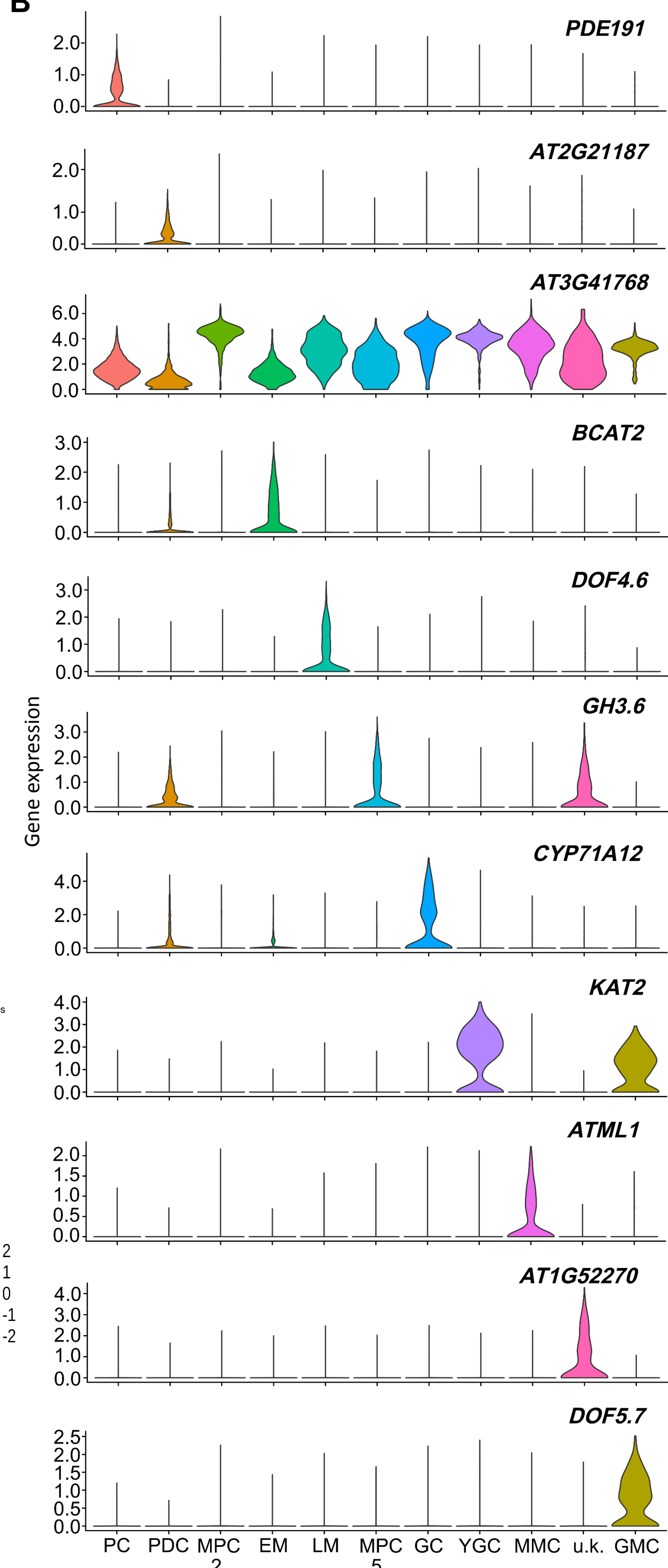
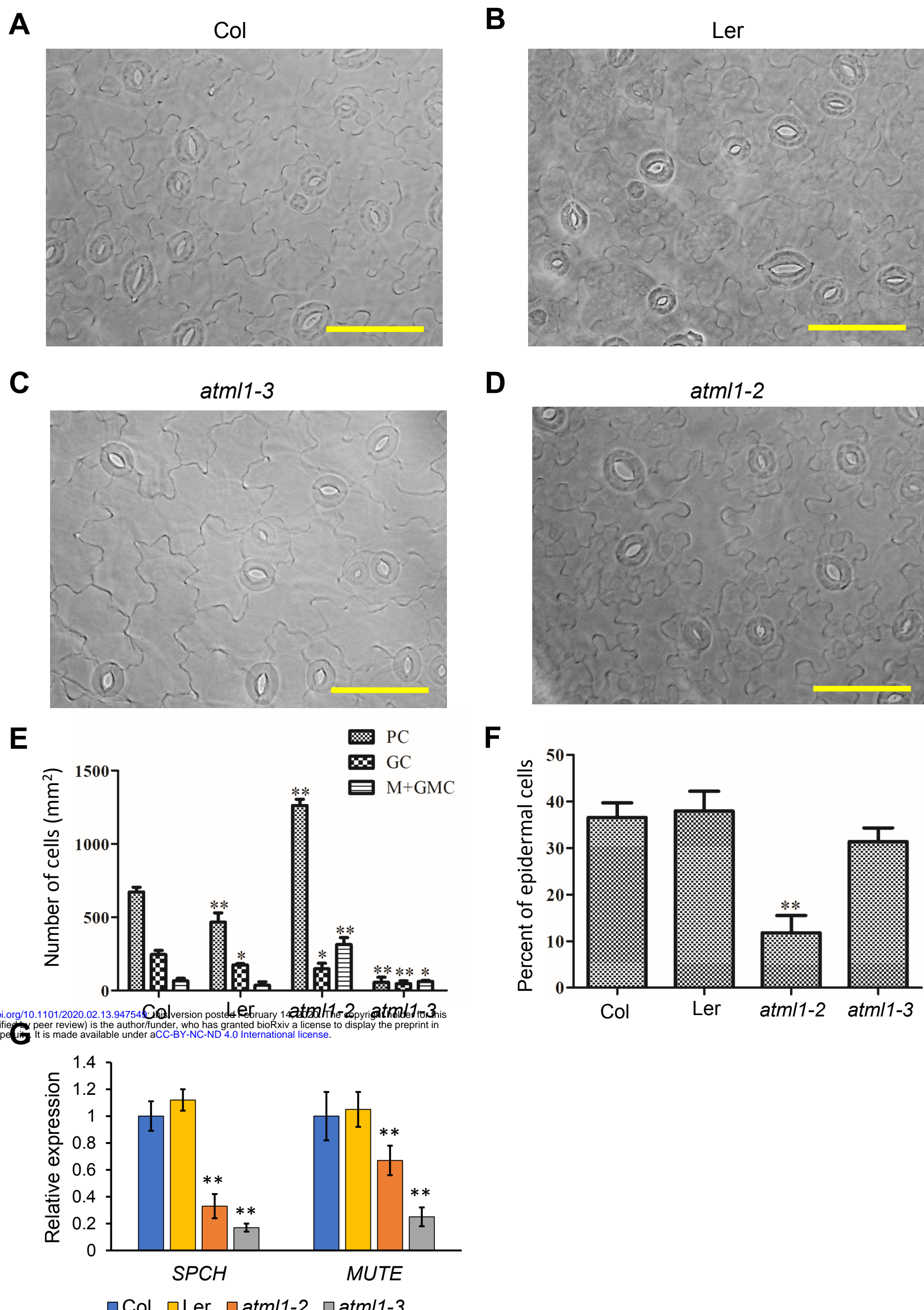
A**B**

Figure 2. Identification of novel marker genes for each cluster. **(A)** Heatmap of expression of representative marker genes in each cluster. **(B)** Violin_plots show expression of representative marker genes in each of cell types. PDC: protodermal cells, PC: pavement cell, M: meristemoid, GMC: guard mother cell, GC: guard cell, MMC: meristemoid mother cell, EM: early stage meristemoid, LM: late stage meristemoid, YGC: young guard cell, MPC: mesophyll cell, u.k. : unknown.



bioRxiv preprint doi: <https://doi.org/10.1101/2020.02.13.947549>; this version posted February 14, 2020. The copyright holder for this preprint (which was not certified by peer review) is the author/funder, who has granted bioRxiv a license to display the preprint in perpetuity. It is made available under aCC-BY-NC-ND 4.0 International license.

Figure 3. ATML1 is involved in regulating the development of stomata. **(A-D)** Analysis of stomatal development of 5-day-old seedlings of *atml1-2* (in Ler background), *atml1-3* (in Col background), Ler and Col are used as controls. **(E-F)** Quantitative analysis of **A-D**. **(G)** qPCR analysis of the expression of *SPCH* and *MUTE* in 5-day-old seedlings of *atml1-2*, *atml1-3*, Ler and Col. Error bars represent standard errors (S.E.). *: $p < 0.05$, **: $p < 0.01$, one-way ANOVA analysis versus Col. Scale bar: 50 μ m in **A-D**.

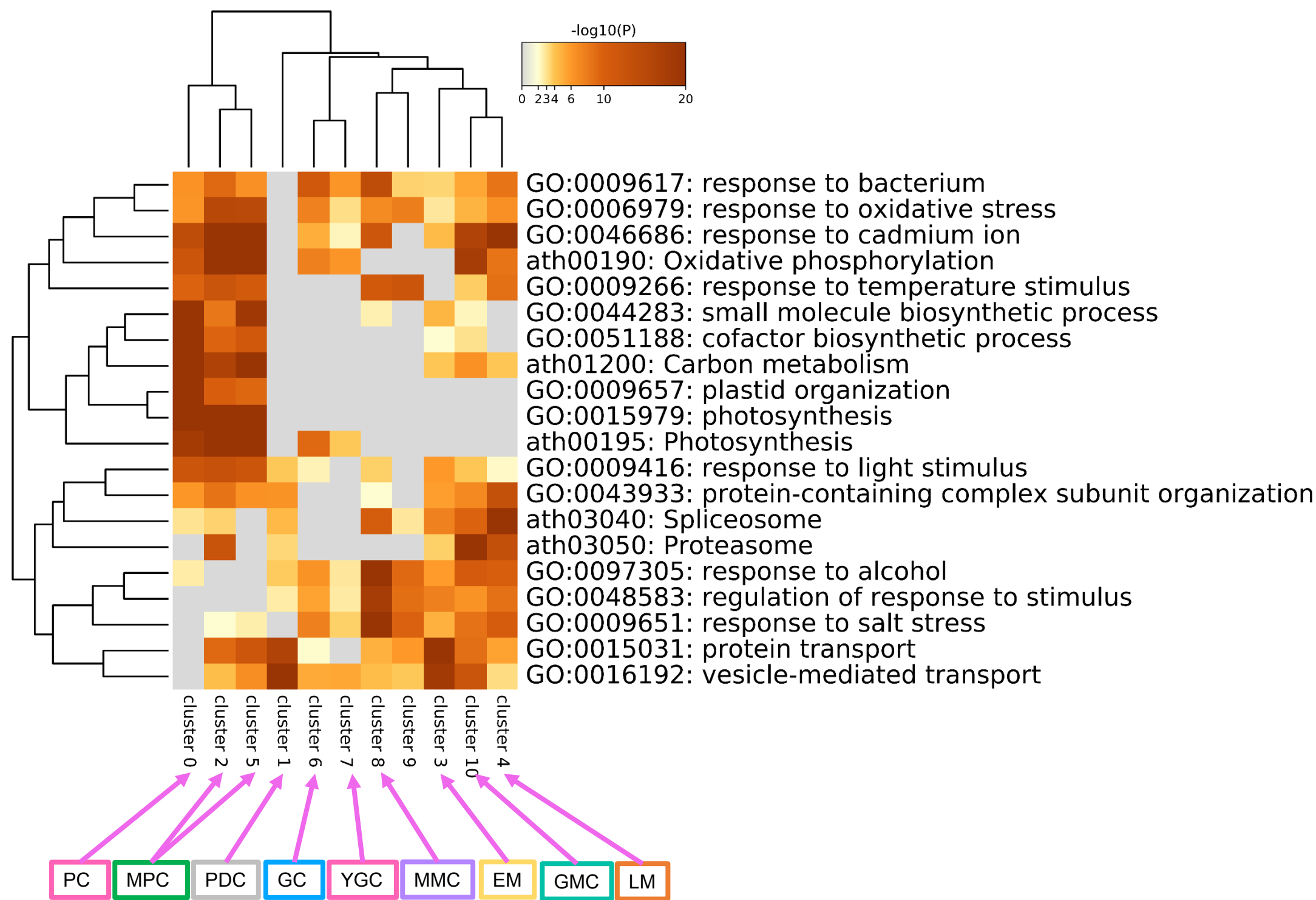
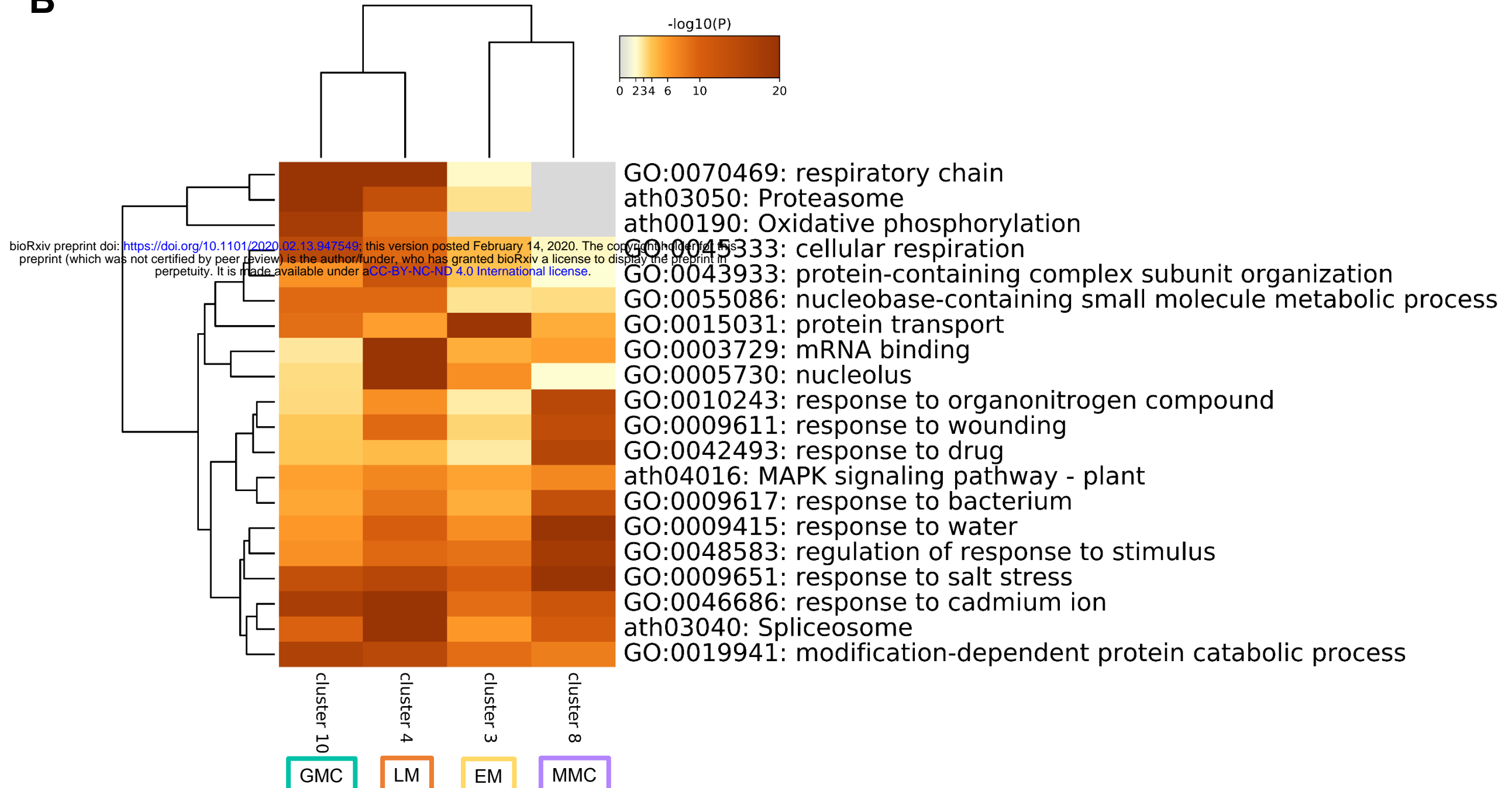
A**B**

Figure 4. GO analysis of the genes that expressed in different cell types. (A) GO-heatmap analysis of the genes with the highest variable expression in different clusters. (B) Same analysis as in A for MMC, GMC, EM and LM.

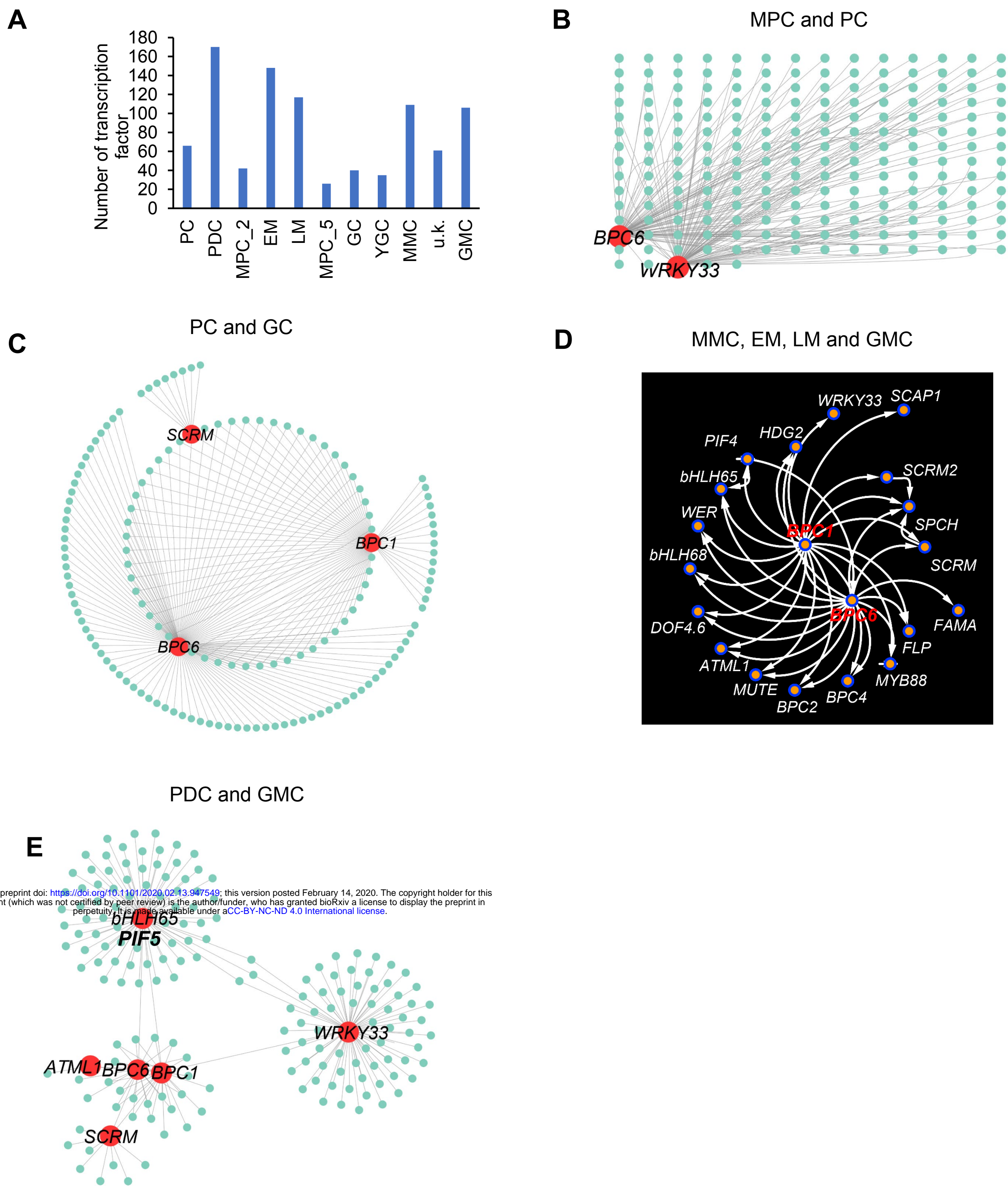


Figure 5. Identification of regulatory networks of transcription factors in different cell types. **(A)** Identification of the transcription factors in different cell types. **(B)** Analysis of the regulatory network of transcription factors in MPC and PC. **(C)** Analysis of the regulatory network of transcription factors in PC and GC. **(D)** Analysis of the regulatory network of transcription factors in MMC, EM, LM and GMC. **(E)** Analysis of the regulatory network of transcription factors in PDC and GMC.

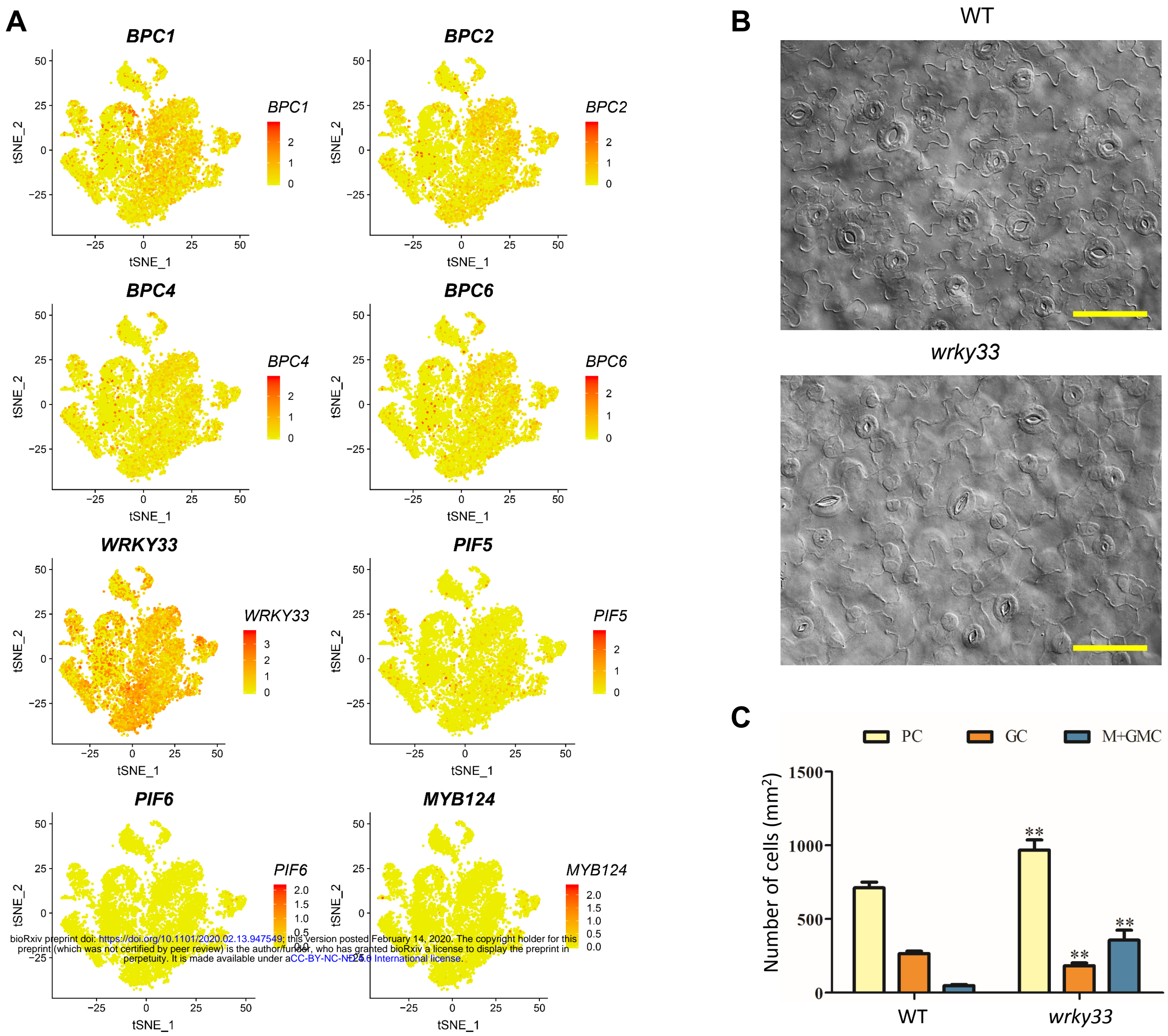
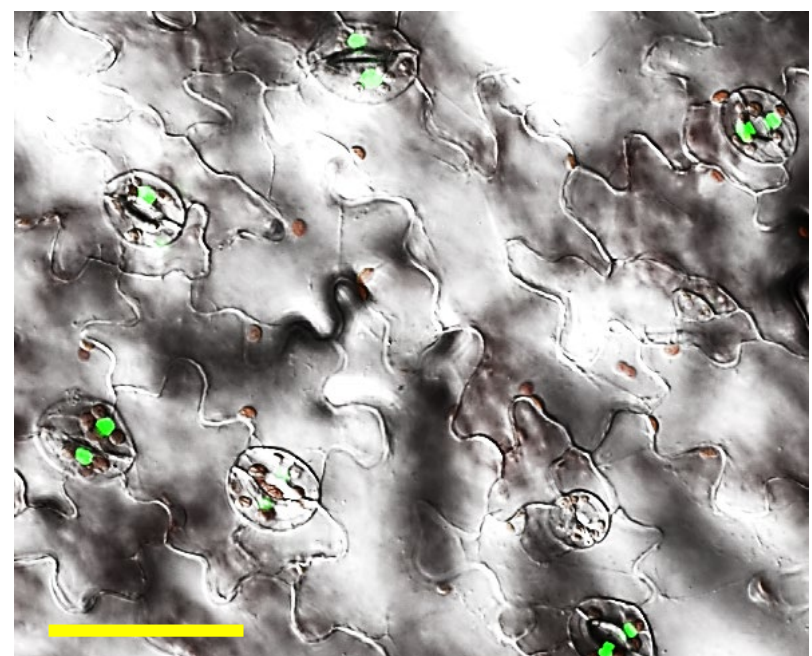
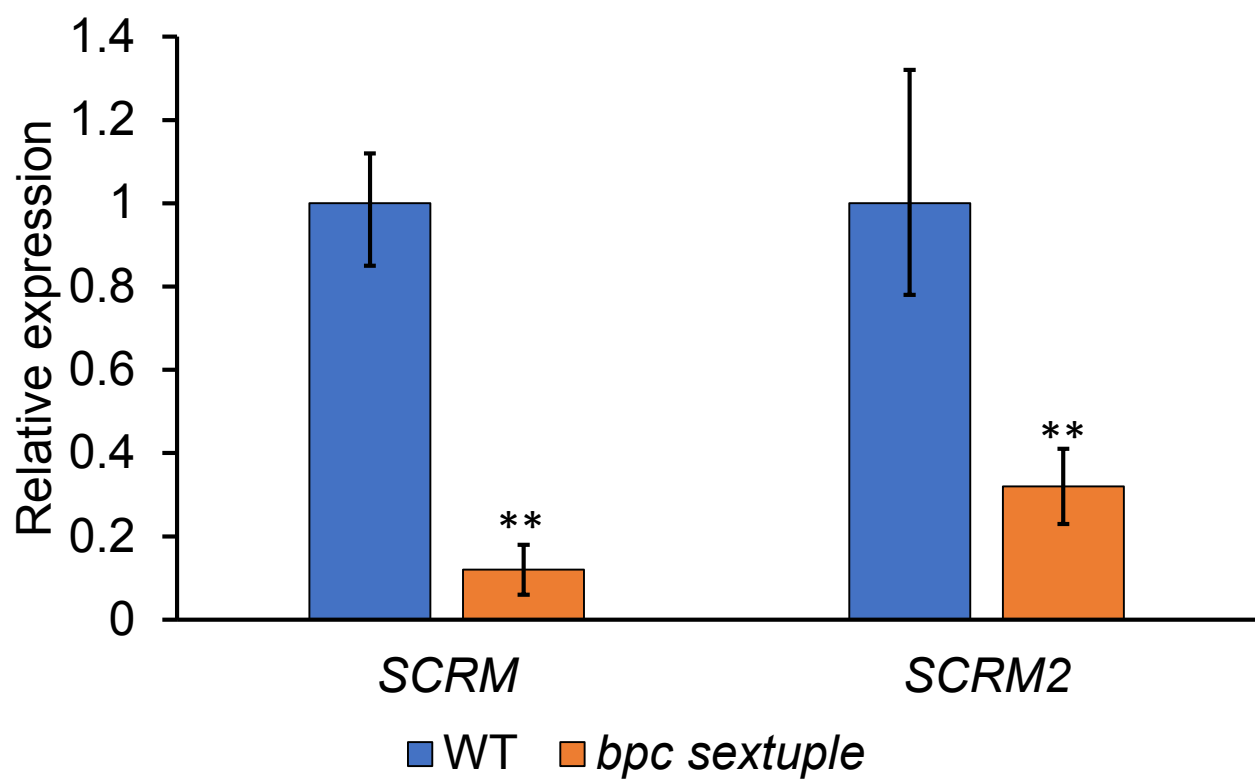
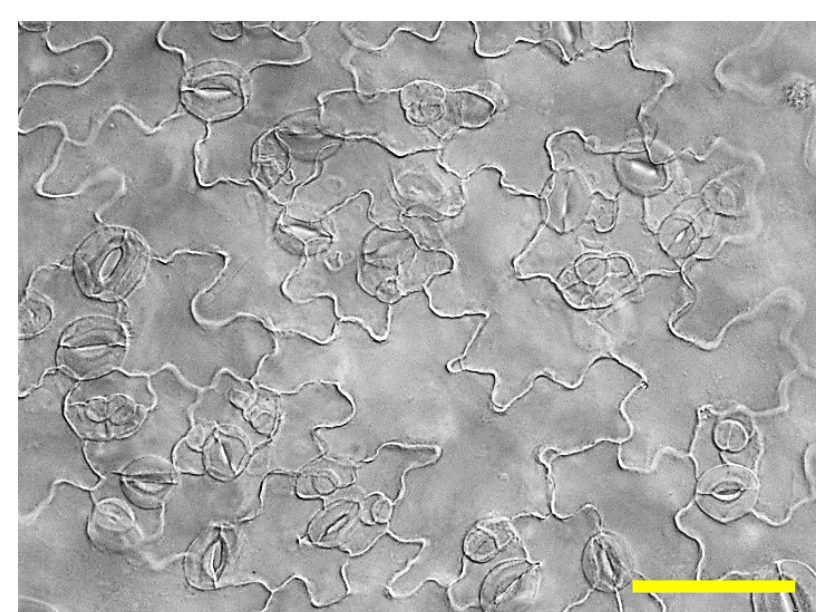
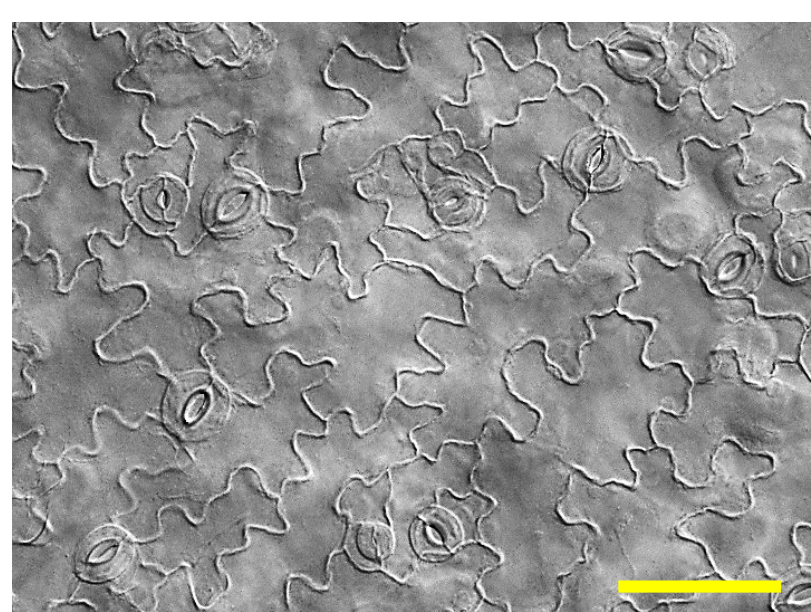
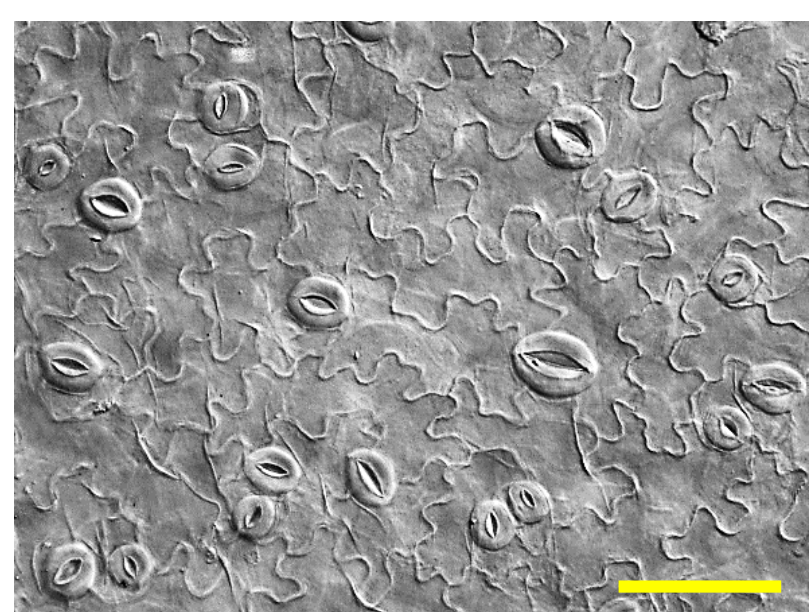
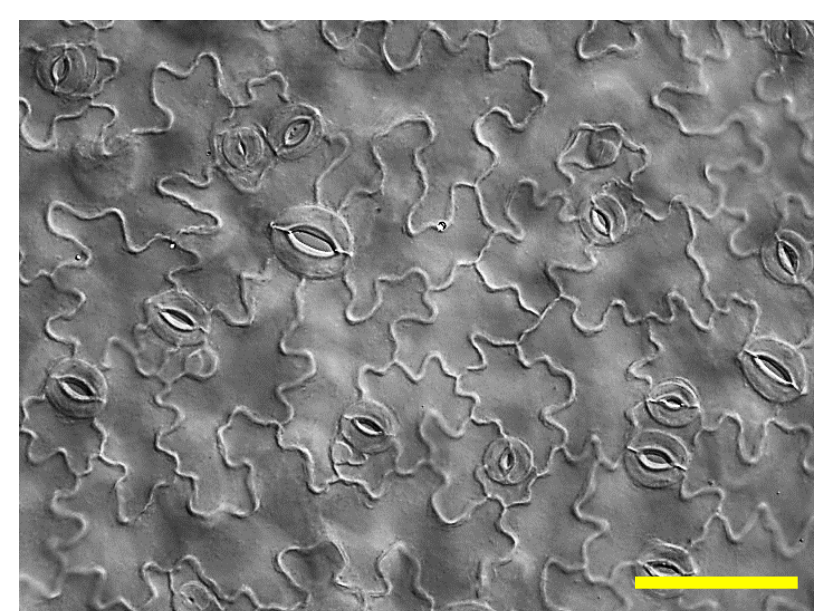
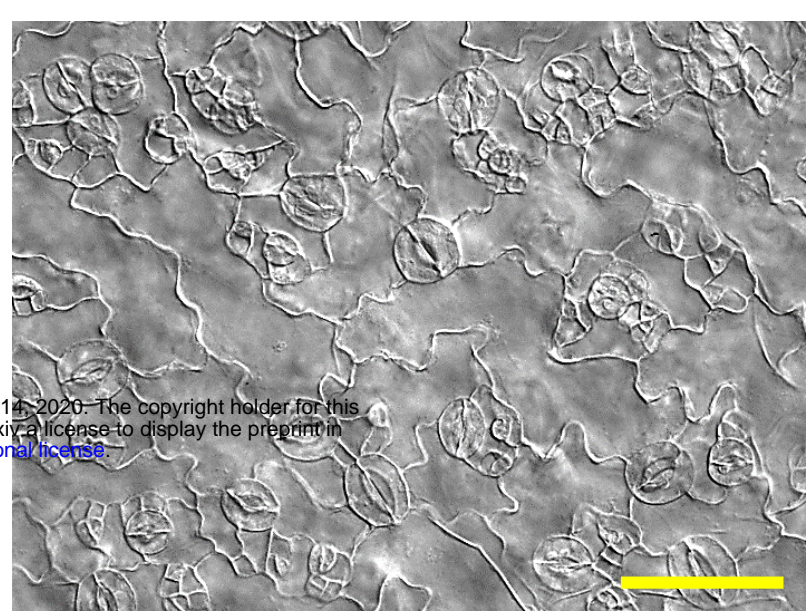
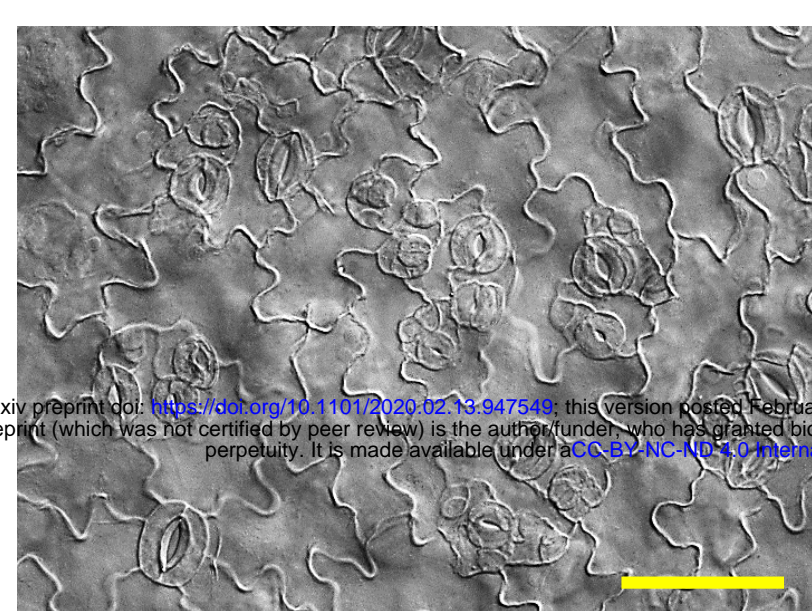


Figure 6. Analysis of feature plots and function of core TFs. **(A)** Feature plots of the expression of representative TFs in different clusters. **(B)** Developmental pattern of stomatal lineage cells of cotyledons of five-day-old seedlings of *wrky33*, with wild type (WT) used as control. **(C)** Frequency of cell types calculated from **(B)**. Error bars represent standard errors (S.E.). *: $p < 0.05$, **: $p < 0.01$, one-way ANOVA analysis versus WT. Scale bar: 50 μ m in **B**.

A*BPC6-GFP***B****C**

WT

*bpc4/6**bpc1/2/3**bpc1/2/4/6**bpc1/2/3/4/6/7**BPC6-GFP*

bioRxiv preprint doi: <https://doi.org/10.1101/2020.02.13.947549>; this version posted February 13, 2020. The copyright holder for this preprint (which was not certified by peer review) is the author/funder, who has granted bioRxiv a license to display the preprint in perpetuity. It is made available under aCC-BY-NC-ND 4.0 International license.

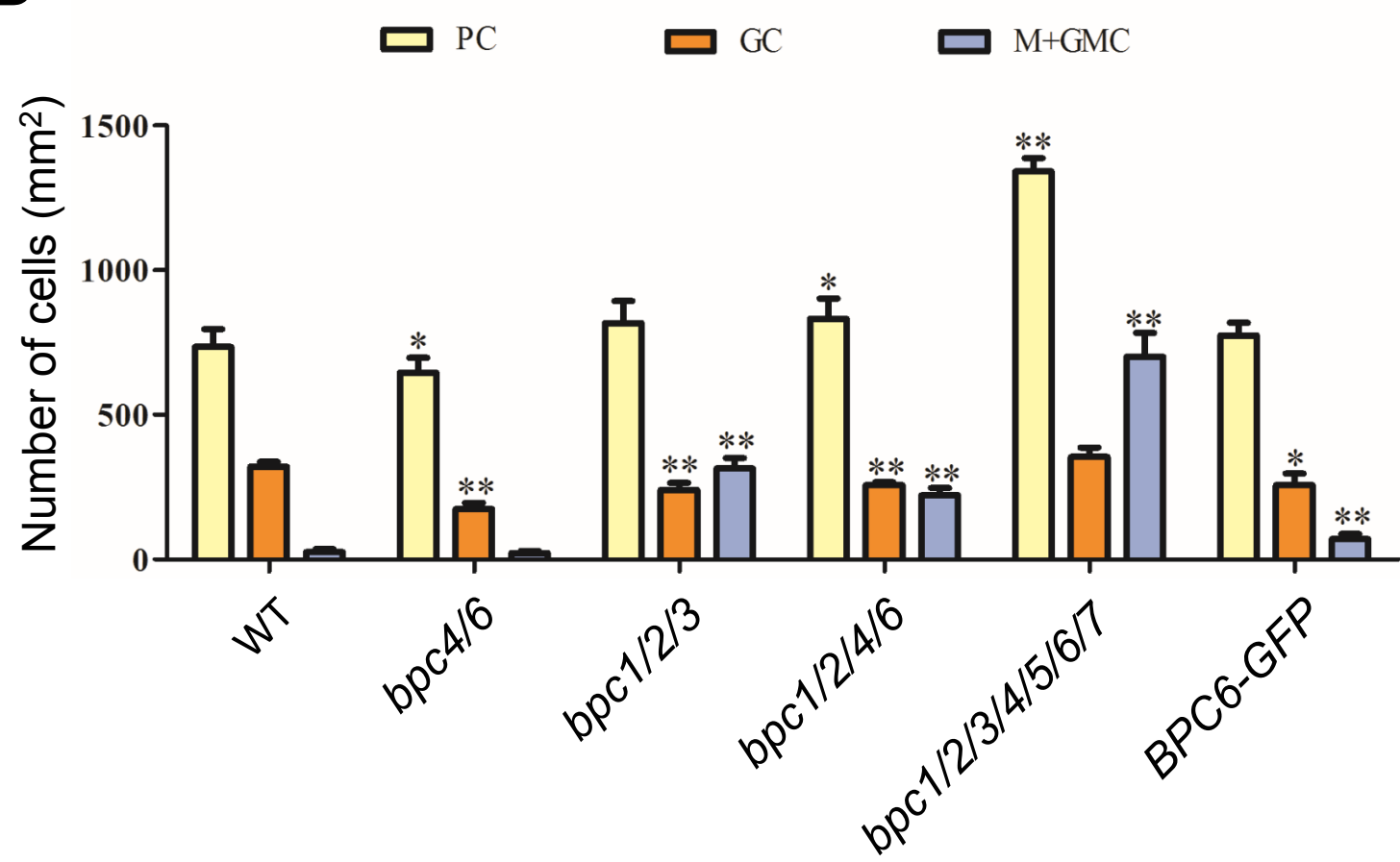
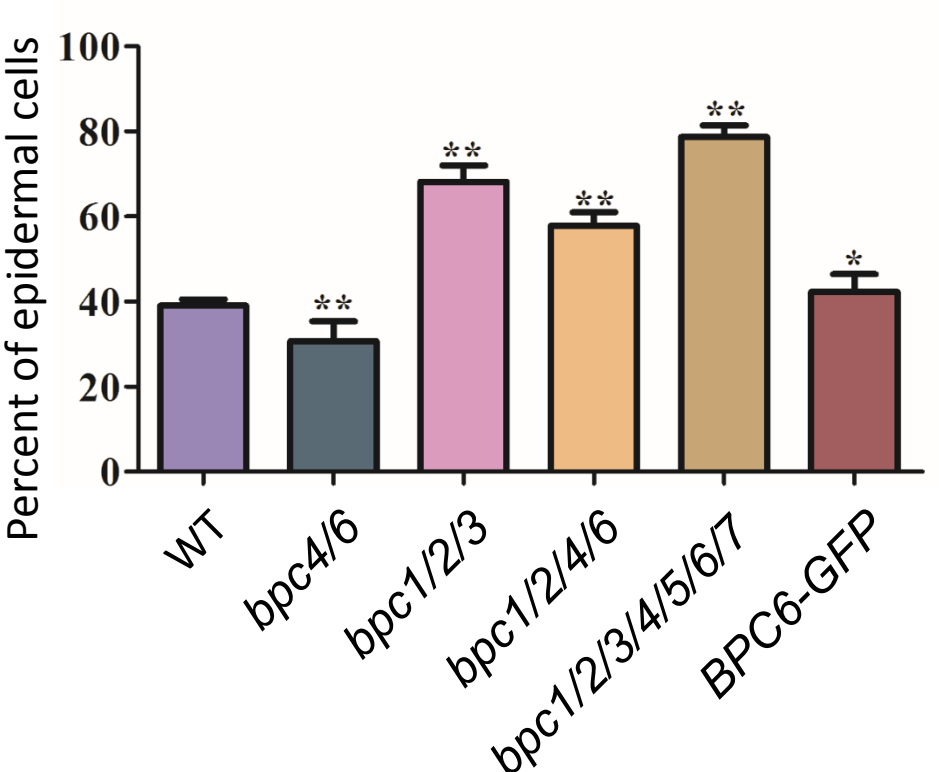
D**E**

Figure 7. BPC proteins are involved in regulating the development of stomata. (A) Analysis of the subcellular localization of BPC6-GFP. **(B)** qPCR analysis of the expression of *SCRM* and *SCRM2* in the *bpc* sextuple mutant. **(C)** Developmental patterns of stomatal lineage cells in cotyledons of 5-day-old seedlings of *bpc* mutants and transgenic plants, WT was use as control. **(D)** Frequency of cell types calculated from (C). **(E)** Number of epidermal cells of mutants grown on MS medium. Error bars represent standard errors (S.E.). *: $p < 0.05$, **: $p < 0.01$, one-way ANOVA analysis versus WT. Scale bar: 50 μ m in A and C.

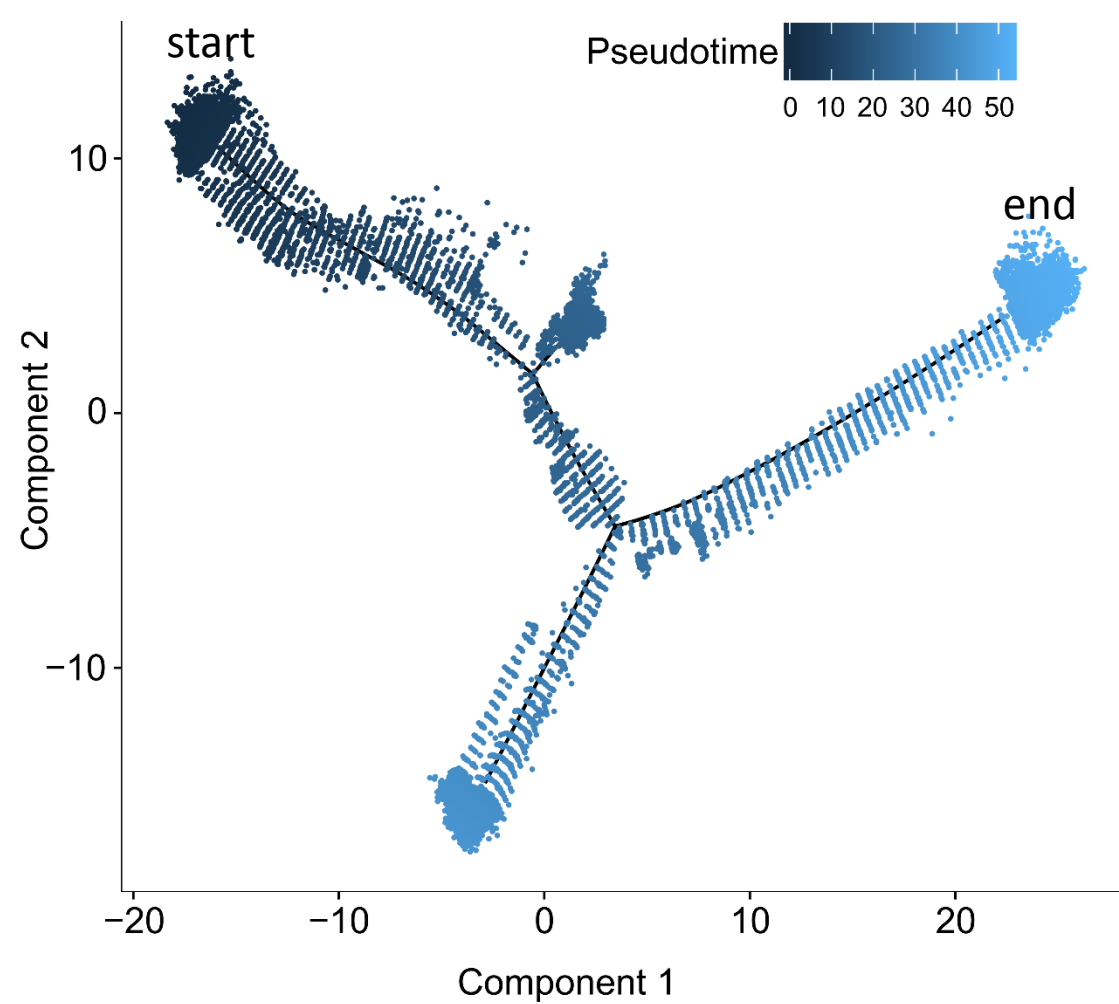
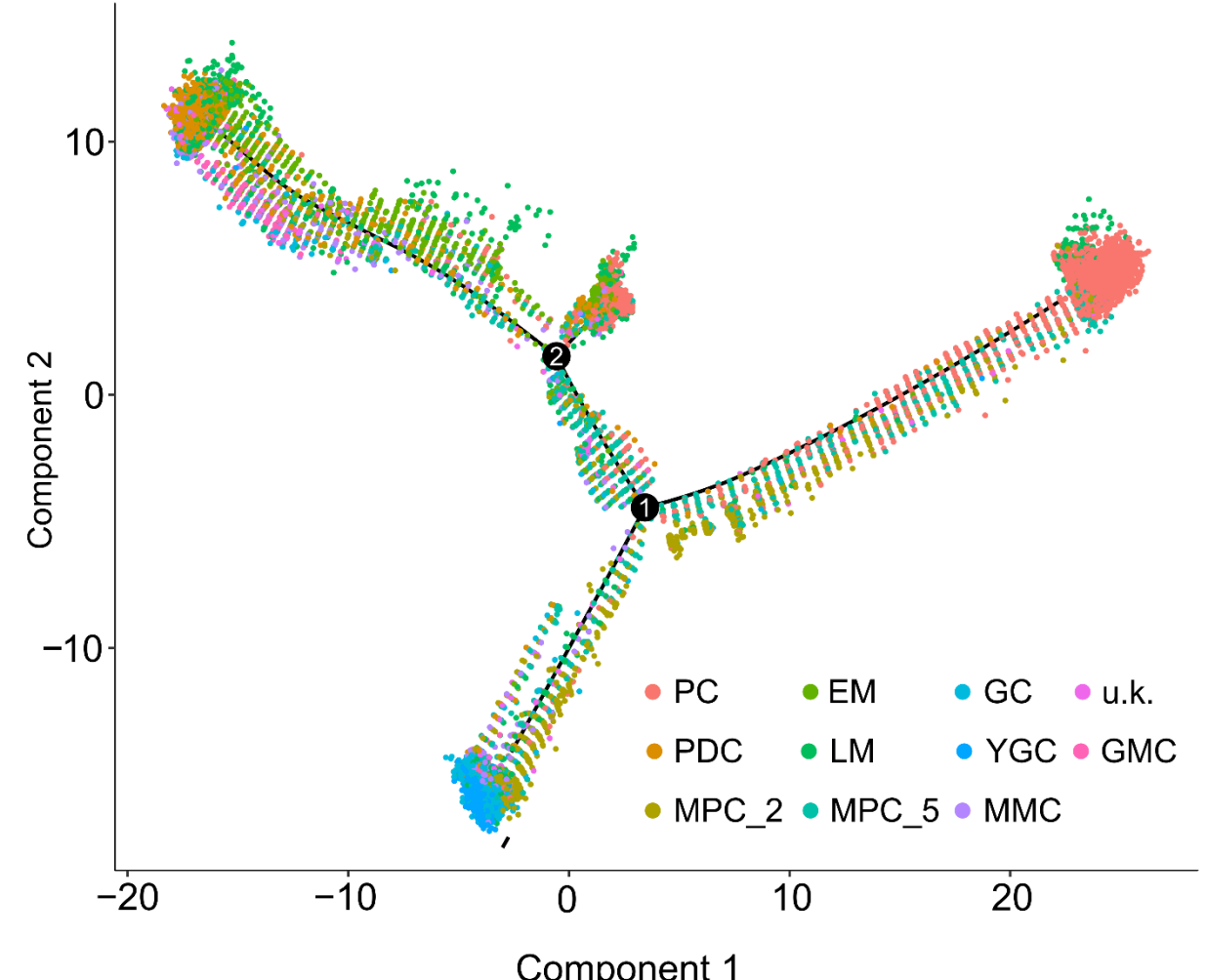
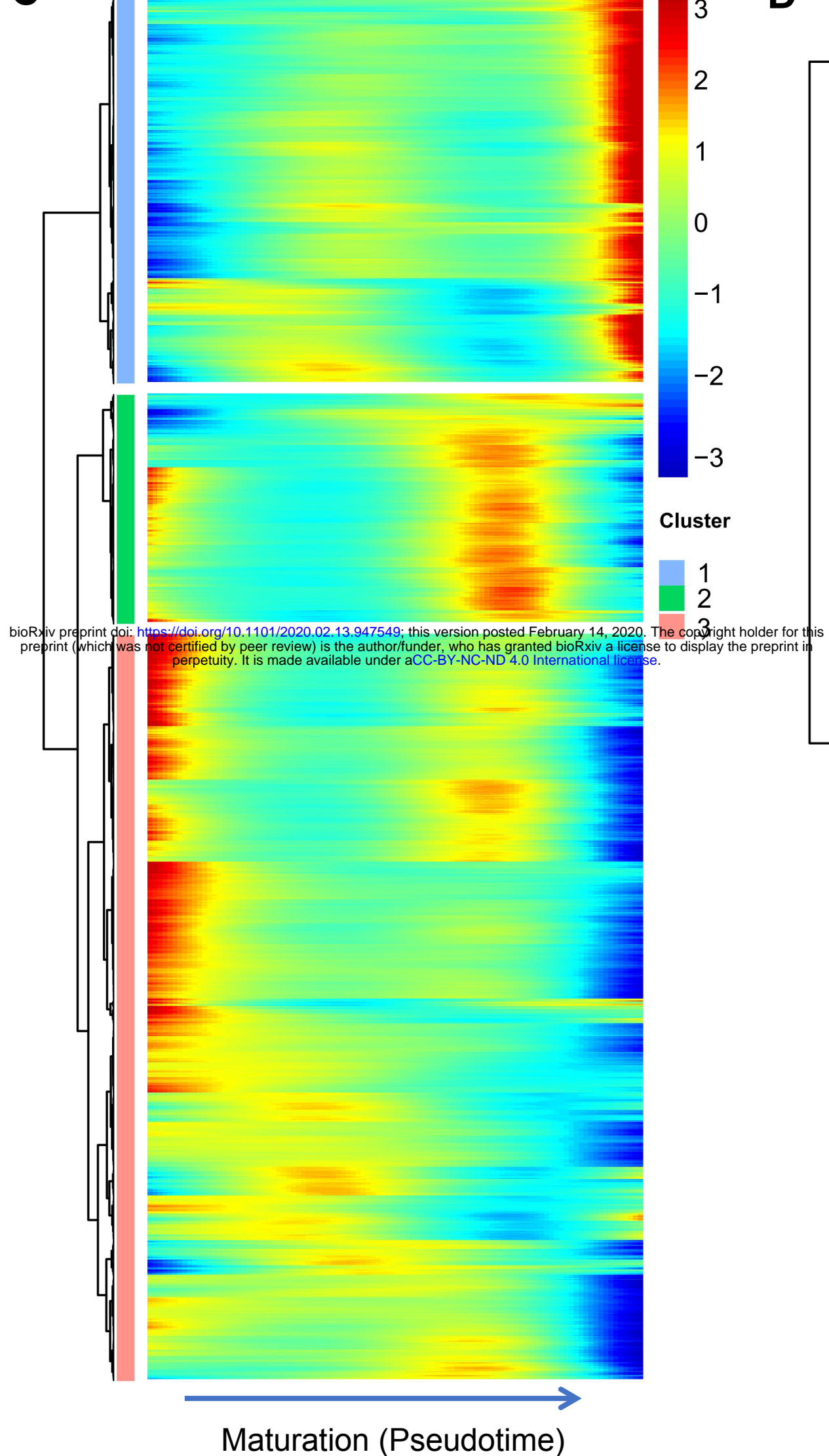
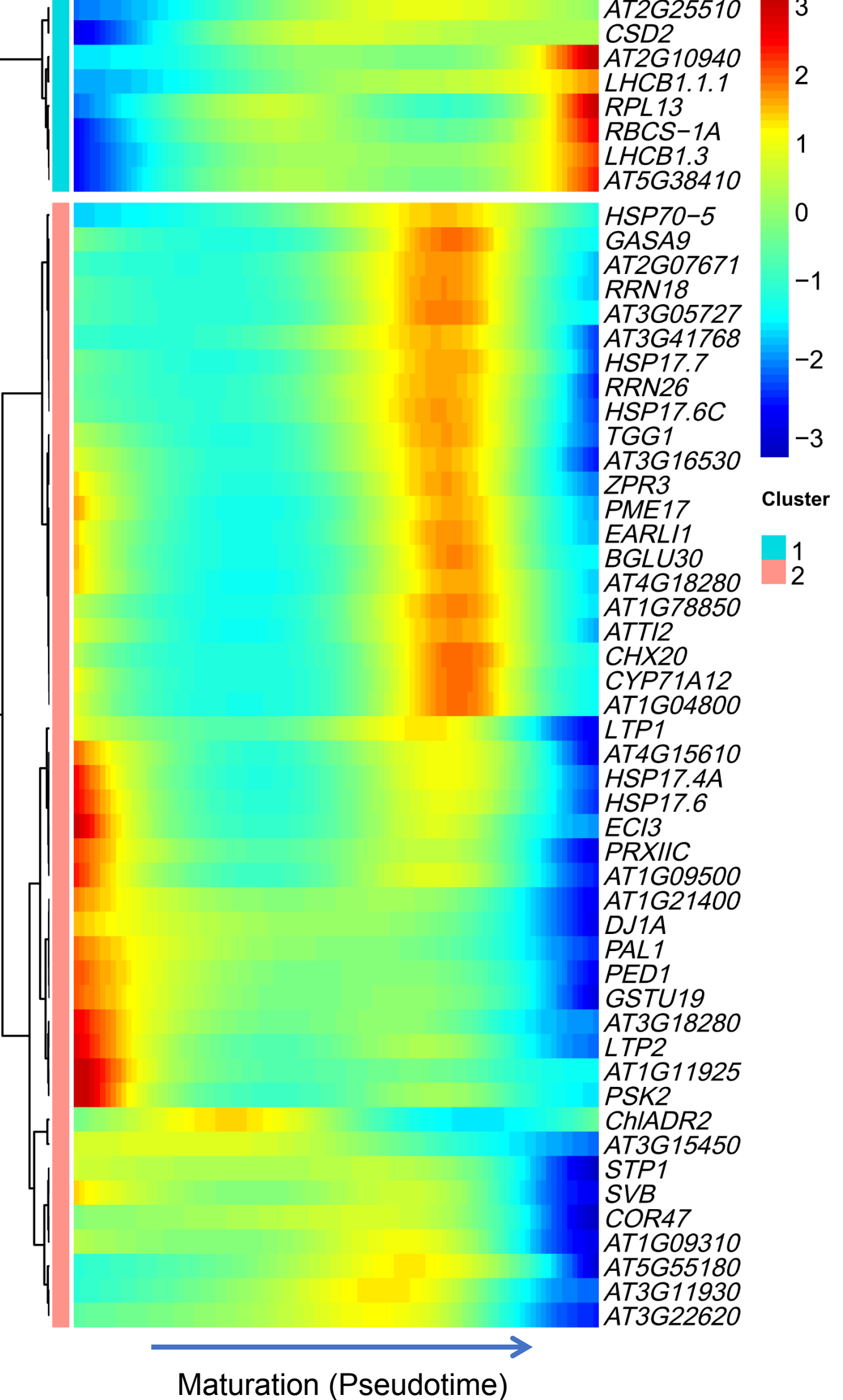
A**B****C****D**

Figure 8. Pseudotime analysis of clusters and the selected marker genes. **(A)** Distribution of cells of each cluster on the pseudotime trajectory. **(B)** Pseudotime trajectory of single-cell transcriptomics data colored according to the cluster labels. Most cells were distributed along main stem, although two small branches were detected near the main path. **(C)** Clustering of all genes during pseudotime progression. **(D)** Clustering and expression kinetics of representative genes along pseudotime progression of stomatal lineage cells.

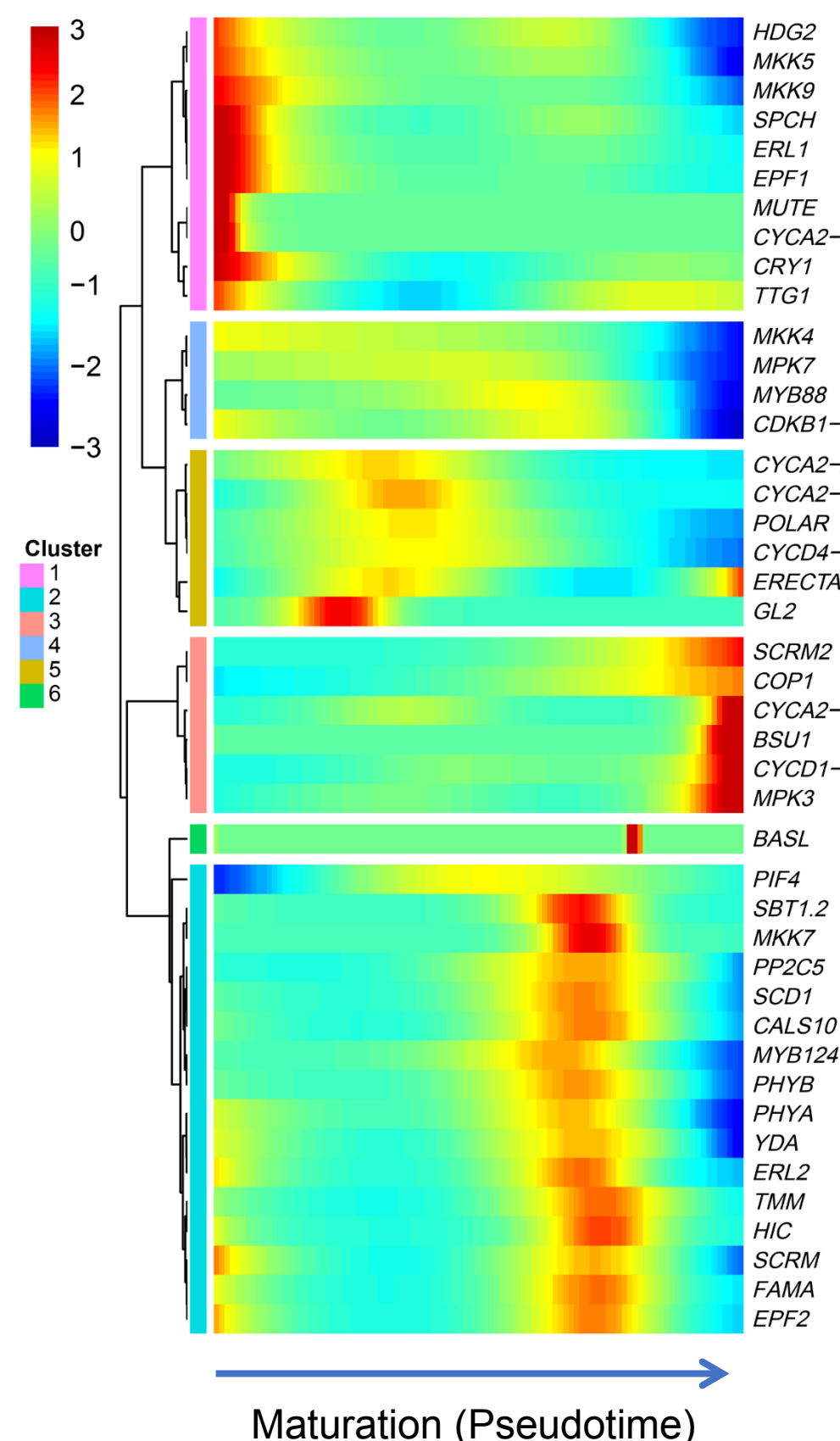
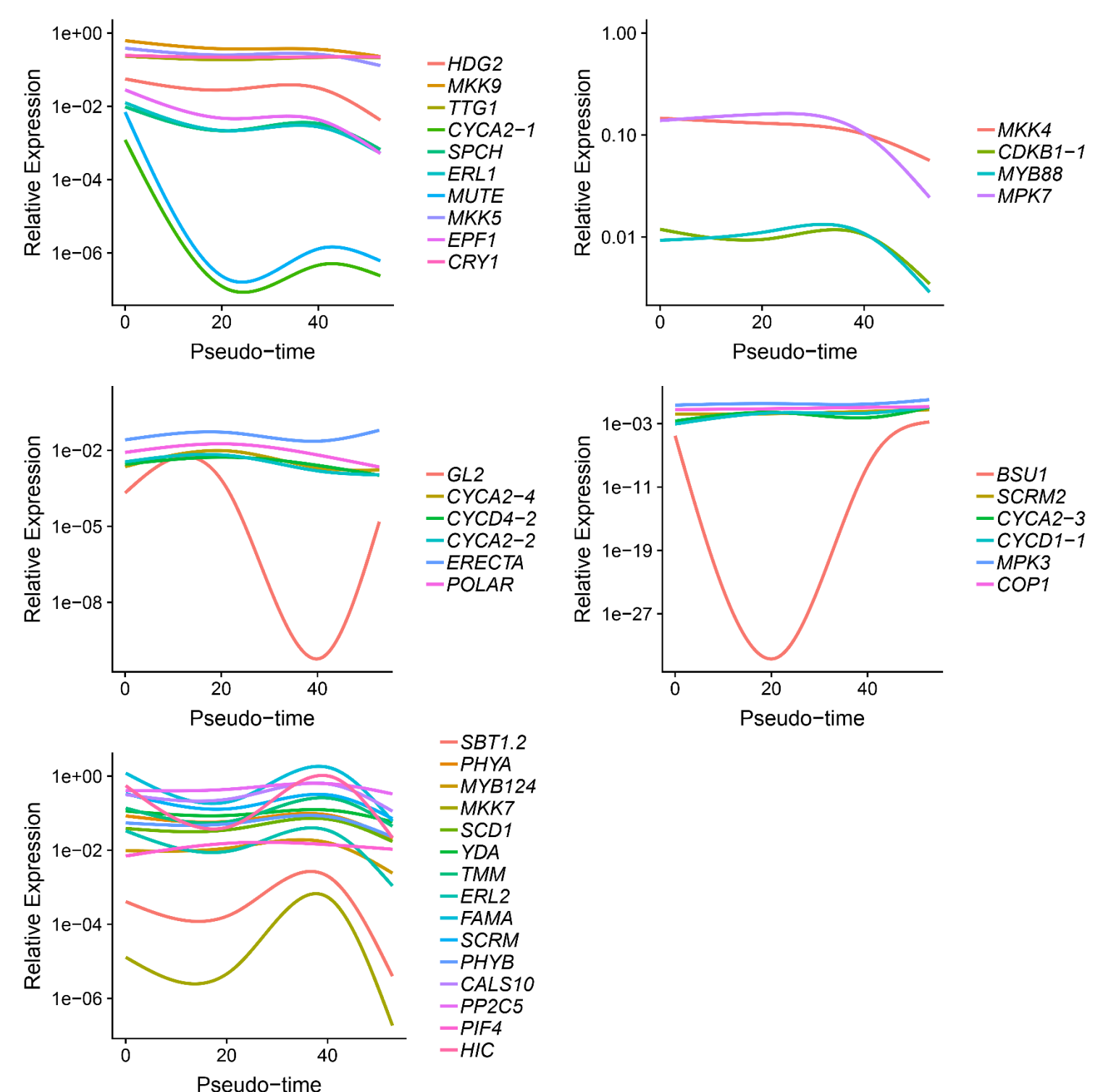
A**B**

Figure 9. Pseudo-time analysis of known marker genes. **(A)** Clustering of representative genes along pseudo-time progression of stomatal lineage cells. **(B)** Gene expression kinetics along pseudo-time progression of representative genes.

bioRxiv preprint doi: <https://doi.org/10.1101/2021.07.14.257109>; this version posted July 14, 2021. The copyright holder for this preprint (which was not certified by peer review) is the author/funder, who has granted bioRxiv a license to display the preprint in perpetuity. It is made available under aCC-BY-NC-ND 4.0 International license.

Parsed Citations

Adrian, J., Chang, J., Ballenger, C.E., Bargmann, B.O.R., Alassimone, J., Davies, K.A., Lau, O.S., Matos, J.L., Hachez, C., Lanctot, A., Vaten, A., Birnbaum, K.D., and Bergmann, D.C. (2015). Transcriptome Dynamics of the Stomatal Lineage: Birth, Amplification, and Termination of a Self-Renewing Population. *Developmental Cell* 33, 107-118.

Pubmed: [Author and Title](#)

Google Scholar: [Author Only](#) [Title Only](#) [Author and Title](#)

Ansbury, S., Hunt, L., Elhaddad, N., Baillie, A., Lundgren, M., Verhertbruggen, Y., Scheller, H.V., Knox, J.P., Fleming, A.J., and Gray, J.E. (2016). Stomatal Function Requires Pectin De-methyl-esterification of the Guard Cell Wall. *Current Biology* 26, 2899-2906.

Pubmed: [Author and Title](#)

Google Scholar: [Author Only](#) [Title Only](#) [Author and Title](#)

Barton, K.A., Schattat, M.H., Jakob, T., Hause, G., Wilhelm, C., McKenna, J.F., Mathe, C., Runions, J., Van Damme, D., and Mathur, J. (2016). Epidermal Pavement Cells of *Arabidopsis* Have Chloroplasts. *Plant Physiol* 171, 723-726.

Pubmed: [Author and Title](#)

Google Scholar: [Author Only](#) [Title Only](#) [Author and Title](#)

Bergmann, D.C., and Sack, F.D. (2007). Stomatal development. *Annu Rev Plant Biol* 58, 163-181.

Pubmed: [Author and Title](#)

Google Scholar: [Author Only](#) [Title Only](#) [Author and Title](#)

Bergmann, D.C., Lukowitz, W., and Somerville, C.R. (2004). Stomatal development and pattern controlled by a MAPKK kinase. *Science* 304, 1494-1497.

Pubmed: [Author and Title](#)

Google Scholar: [Author Only](#) [Title Only](#) [Author and Title](#)

Biggin, M.D., and Tjian, R. (1988). Transcription factors that activate the Ultrabithorax promoter in developmentally staged extracts. *Cell* 53, 699-711.

Pubmed: [Author and Title](#)

Google Scholar: [Author Only](#) [Title Only](#) [Author and Title](#)

Casson, S.A., Franklin, K.A., Gray, J.E., Grierson, C.S., Whitelam, G.C., and Hetherington, A.M. (2009). phytochrome B and PIF4 Regulate Stomatal Development in Response to Light Quantity. *Current Biology* 19, 229-234.

Pubmed: [Author and Title](#)

Google Scholar: [Author Only](#) [Title Only](#) [Author and Title](#)

Chanroj, S., Padmanaban, S., Czerny, D.D., Jauh, G.Y., and Sze, H. (2013). K⁺ transporter AtCHX17 with its hydrophilic C tail localizes to membranes of the secretory/endocytic system: role in reproduction and seed set. *Mol Plant* 6, 1226-1246.

Pubmed: [Author and Title](#)

Google Scholar: [Author Only](#) [Title Only](#) [Author and Title](#)

Chen, L., Guan, L.P., Qian, P.P., Xu, F., Wu, Z.L., Wu, Y.J., He, K., Gou, X.P., Li, J., and Hou, S.W. (2016). NRPB3, the third largest subunit of RNA polymerase II, is essential for stomatal patterning and differentiation in *Arabidopsis*. *Development* 143, 1600-1611.

Pubmed: [Author and Title](#)

Google Scholar: [Author Only](#) [Title Only](#) [Author and Title](#)

Dong, J., MacAlister, C.A., and Bergmann, D.C. (2009). BASL controls asymmetric cell division in *Arabidopsis*. *Cell* 137, 1320-1330.

Pubmed: [Author and Title](#)

Google Scholar: [Author Only](#) [Title Only](#) [Author and Title](#)

Dutton, C., Horak, H., Hepworth, C., Mitchell, A., Ton, J., Hunt, L., and Gray, J.E. (2019). Bacterial infection systemically suppresses stomatal density. *Plant Cell Environ* 42, 2411-2421.

Pubmed: [Author and Title](#)

Google Scholar: [Author Only](#) [Title Only](#) [Author and Title](#)

Engineer, C.B., Ghassemian, M., Anderson, J.C., Peck, S.C., Hu, H.H., and Schroeder, J.I. (2015). Carbonic anhydrases, EPF2 and a novel protease mediate CO₂ control of stomatal development (vol 513, pg 246, 2014). *Nature* 526, 458-458.

Pubmed: [Author and Title](#)

Google Scholar: [Author Only](#) [Title Only](#) [Author and Title](#)

Fu, C., Hou, Y., Ge, J., Zhang, L., Liu, X., Huo, P., and Liu, J. (2019). Increased fes1a thermotolerance is induced by BAG6 knockout. *Plant Mol Biol* 100, 73-82.

Pubmed: [Author and Title](#)

Google Scholar: [Author Only](#) [Title Only](#) [Author and Title](#)

Fu, Y., Gu, Y., Zheng, Z., Wasteneys, G., and Yang, Z (2005). *Arabidopsis* interdigitating cell growth requires two antagonistic pathways with opposing action on cell morphogenesis. *Cell* 120, 687-700.

Pubmed: [Author and Title](#)

Google Scholar: [Author Only](#) [Title Only](#) [Author and Title](#)

Geisler, M., Nadeau, J., and Sack, F.D. (2000). Oriented asymmetric divisions that generate the stomatal spacing pattern in *Arabidopsis* are disrupted by the too many mouths mutation. *Plant Cell* 12, 2075-2086.

Pubmed: [Author and Title](#)

Google Scholar: [Author Only](#) [Title Only](#) [Author and Title](#)

Gray, J. (2005). Guard cells: transcription factors regulate stomatal movements. *Curr Biol* 15, R593-595.

Pubmed: [Author and Title](#)

Google Scholar: [Author Only](#) [Title Only](#) [Author and Title](#)

Han, S.K., and Torii, K.U. (2016). Lineage-specific stem cells, signals and asymmetries during stomatal development. *Development* 143, 1259-1270.

Pubmed: [Author and Title](#)

Google Scholar: [Author Only](#) [Title Only](#) [Author and Title](#)

Han, S.K., Qi, X., Sugihara, K., Dang, J.H., Endo, T.A., Miller, K.L., Kim, E.D., Miura, T., and Torii, K.U. (2018). MUTE Directly Orchestrates Cell-State Switch and the Single Symmetric Division to Create Stomata. *Dev Cell* 45, 303-315 e305.

Pubmed: [Author and Title](#)

Google Scholar: [Author Only](#) [Title Only](#) [Author and Title](#)

Hara, K., Kajita, R., Torii, K.U., Bergmann, D.C., and Kakimoto, T. (2007). The secretory peptide gene EPF1 enforces the stomatal one-cell-spacing rule. *Gene Dev* 21, 1720-1725.

Pubmed: [Author and Title](#)

Google Scholar: [Author Only](#) [Title Only](#) [Author and Title](#)

Hronkova, M., Wiesnerova, D., Simkova, M., Skupa, P., Dewitte, W., Vrablova, M., Zazimalova, E., and Santrucek, J. (2015). Light-induced STOMAGEN-mediated stomatal development in *Arabidopsis* leaves. *Journal of Experimental Botany* 66, 4621-4630.

Pubmed: [Author and Title](#)

Google Scholar: [Author Only](#) [Title Only](#) [Author and Title](#)

Huang, S., Waadt, R., Nuhkat, M., Kollist, H., Hedrich, R., and Roelfsema, M.R.G. (2019). Ca(2+) signals in guard cells enhance the efficiency by which ABA triggers stomatal closure. *New Phytol.*

Pubmed: [Author and Title](#)

Google Scholar: [Author Only](#) [Title Only](#) [Author and Title](#)

Hunt, L., and Gray, J.E. (2009a). The signaling peptide EPF2 controls asymmetric cell divisions during stomatal development. *Curr Biol* 19, 864-869.

Pubmed: [Author and Title](#)

Google Scholar: [Author Only](#) [Title Only](#) [Author and Title](#)

Hunt, L., and Gray, J.E. (2009b). The Signaling Peptide EPF2 Controls Asymmetric Cell Divisions during Stomatal Development. *Current Biology* 19, 864-869.

Pubmed: [Author and Title](#)

Google Scholar: [Author Only](#) [Title Only](#) [Author and Title](#)

Iida, H., Yoshida, A., and Takada, S. (2019). ATML1 activity is restricted to the outermost cells of the embryo through post-transcriptional repressions. *Development* 146.

Pubmed: [Author and Title](#)

Google Scholar: [Author Only](#) [Title Only](#) [Author and Title](#)

Kabbage, M., and Dickman, M.B. (2008). The BAG proteins: a ubiquitous family of chaperone regulators. *Cell Mol Life Sci* 65, 1390-1402.

Pubmed: [Author and Title](#)

Google Scholar: [Author Only](#) [Title Only](#) [Author and Title](#)

Kanaoka, M.M., Pillitteri, L.J., Fujii, H., Yoshida, Y., Bogenschutz, N.L., Takabayashi, J., Zhu, J.K., and Torii, K.U. (2008). SCREAM/ICE1 and SCREAM2 specify three cell-state transitional steps leading to *Arabidopsis* stomatal differentiation. *Plant Cell* 20, 1775-1785.

Pubmed: [Author and Title](#)

Google Scholar: [Author Only](#) [Title Only](#) [Author and Title](#)

Kang, C.Y., Lian, H.L., Wang, F.F., Huang, J.R., and Yang, H.Q. (2009). Cryptochromes, Phytochromes, and COP1 Regulate Light-Controlled Stomatal Development in *Arabidopsis*. *Plant Cell* 21, 2624-2641.

Pubmed: [Author and Title](#)

Google Scholar: [Author Only](#) [Title Only](#) [Author and Title](#)

Kim, T.W., Michniewicz, M., Bergmann, D.C., and Wang, Z.Y. (2012). Brassinosteroid regulates stomatal development by GSK3-mediated inhibition of a MAPK pathway. *Nature* 482, 419-U1526.

Pubmed: [Author and Title](#)

Google Scholar: [Author Only](#) [Title Only](#) [Author and Title](#)

Kooiker, M., Airoldi, C.A., Losa, A., Manzotti, P.S., Finzi, L., Kater, M.M., and Colombo, L. (2005). BASIC PENTACysteine1, a GA binding protein that induces conformational changes in the regulatory region of the homeotic *Arabidopsis* gene SEEDSTICK. *Plant Cell* 17, 722-729.

Pubmed: [Author and Title](#)

Google Scholar: [Author Only](#) [Title Only](#) [Author and Title](#)

Lai, L.B., Nadeau, J.A., Lucas, J., Lee, E.K., Nakagawa, T., Zhao, L.M., Geisler, M., and Sack, F.D. (2005). The *Arabidopsis* R2R3 MYB proteins FOUR LIPS and MYB88 restrict divisions late in the stomatal cell lineage. *Plant Cell* 17, 2754-2767.

Pubmed: [Author and Title](#)

Google Scholar: [Author Only](#) [Title Only](#) [Author and Title](#)

Lampard, G.R., MacAlister, C.A., and Bergmann, D.C. (2008). Arabidopsis Stomatal Initiation Is Controlled by MAPK-Mediated Regulation of the bHLH SPEECHLESS. *Science* 322, 1113-1116.

Pubmed: [Author and Title](#)

Google Scholar: [Author Only](#) [Title Only](#) [Author and Title](#)

Lampard, G.R., Lukowitz, W., Ellis, B.E., and Bergmann, D.C. (2009). Novel and Expanded Roles for MAPK Signaling in Arabidopsis Stomatal Cell Fate Revealed by Cell Type-Specific Manipulations. *Plant Cell* 21, 3506-3517.

Pubmed: [Author and Title](#)

Google Scholar: [Author Only](#) [Title Only](#) [Author and Title](#)

Lawson, T. (2009). Guard cell photosynthesis and stomatal function. *New Phytol* 181, 13-34.

Pubmed: [Author and Title](#)

Google Scholar: [Author Only](#) [Title Only](#) [Author and Title](#)

Lee, J.S., Hnilova, M., Maes, M., Lin, Y.C.L., Putarjunan, A., Han, S.K., Avila, J., and Torii, K.U. (2015). Competitive binding of antagonistic peptides fine-tunes stomatal patterning. *Nature* 522, 435-+.

Pubmed: [Author and Title](#)

Google Scholar: [Author Only](#) [Title Only](#) [Author and Title](#)

Lee, J.S., Kuroha, T., Hnilova, M., Khatayevich, D., Kanaoka, M.M., McAbee, J.M., Sarikaya, M., Tamerler, C., and Torii, K.U. (2012). Direct interaction of ligand-receptor pairs specifying stomatal patterning. *Gene Dev* 26, 126-136.

Pubmed: [Author and Title](#)

Google Scholar: [Author Only](#) [Title Only](#) [Author and Title](#)

Lee, J.Y., Colinas, J., Wang, J.Y., Mace, D., Ohler, U., and Benfey, P.N. (2006). Transcriptional and posttranscriptional regulation of transcription factor expression in *Arabidopsis* roots. *Proc Natl Acad Sci U S A* 103, 6055-6060.

Pubmed: [Author and Title](#)

Google Scholar: [Author Only](#) [Title Only](#) [Author and Title](#)

Lehmann, M. (2004). Anything else but GAGA: a nonhistone protein complex reshapes chromatin structure. *Trends in genetics : TIG* 20, 15-22.

Pubmed: [Author and Title](#)

Google Scholar: [Author Only](#) [Title Only](#) [Author and Title](#)

Li, J., Brader, G., and Palva, E.T. (2008). Kunitz trypsin inhibitor: an antagonist of cell death triggered by phytopathogens and fumonisin b1 in *Arabidopsis*. *Mol Plant* 1, 482-495.

Pubmed: [Author and Title](#)

Google Scholar: [Author Only](#) [Title Only](#) [Author and Title](#)

Li, Y., Kabbage, M., Liu, W., and Dickman, M.B. (2016). Aspartyl Protease-Mediated Cleavage of BAG6 Is Necessary for Autophagy and Fungal Resistance in Plants. *Plant Cell* 28, 233-247.

Pubmed: [Author and Title](#)

Google Scholar: [Author Only](#) [Title Only](#) [Author and Title](#)

Liang, H., Zhang, Y., Martinez, P., Rasmussen, C.G., Xu, T., and Yang, Z (2018). The Microtubule-Associated Protein IQ67 DOMAIN5 Modulates Microtubule Dynamics and Pavement Cell Shape. *Plant Physiol* 177, 1555-1568.

Pubmed: [Author and Title](#)

Google Scholar: [Author Only](#) [Title Only](#) [Author and Title](#)

MacAlister, C.A., Ohashi-Ito, K., and Bergmann, D.C. (2007). Transcription factor control of asymmetric cell divisions that establish the stomatal lineage. *Nature* 445, 537-540.

Pubmed: [Author and Title](#)

Google Scholar: [Author Only](#) [Title Only](#) [Author and Title](#)

Macosko, E.Z., Basu, A., Satija, R., Nemesh, J., Shekhar, K., Goldman, M., Tirosh, I., Bialas, A.R., Kamitaki, N., Martersteck, E.M., Trombetta, J.J., Weitz, D.A., Sanes, J.R., Shalek, A.K., Regev, A., and McCarroll, S.A (2015). Highly Parallel Genome-wide Expression Profiling of Individual Cells Using Nanoliter Droplets. *Cell* 161, 1202-1214.

Pubmed: [Author and Title](#)

Google Scholar: [Author Only](#) [Title Only](#) [Author and Title](#)

Maresova, L., and Sychrova, H. (2006). *Arabidopsis thaliana* CHX17 gene complements the kha1 deletion phenotypes in *Saccharomyces cerevisiae*. *Yeast* 23, 1167-1171.

Pubmed: [Author and Title](#)

Google Scholar: [Author Only](#) [Title Only](#) [Author and Title](#)

Melotto, M., Underwood, W., Koczan, J., Nomura, K., and He, S.Y. (2006). Plant stomata function in innate immunity against bacterial invasion. *Cell* 126, 969-980.

Pubmed: [Author and Title](#)

Google Scholar: [Author Only](#) [Title Only](#) [Author and Title](#)

Monfared, M.M., Simon, M.K., Meister, R.J., Roig-Villanova, I., Kooiker, M., Colombo, L., Fletcher, J.C., and Gasser, C.S. (2011). Overlapping and antagonistic activities of BASIC PENTACSTEINE genes affect a range of developmental processes in *Arabidopsis*. *Plant J* 66, 1020-1031.

Pubmed: [Author and Title](#)

Google Scholar: [Author Only](#) [Title Only](#) [Author and Title](#)

Mu, Y., Zou, M., Sun, X., He, B., Xu, X., Liu, Y., Zhang, L., and Chi, W. (2017). BASIC PENTACSTEINE Proteins Repress ABSCISIC ACID INSENSITIVE4 Expression via Direct Recruitment of the Polycomb-Repressive Complex 2 in Arabidopsis Root Development. *Plant Cell Physiol* 58, 607-621.

Pubmed: [Author and Title](#)

Google Scholar: [Author Only](#) [Title Only](#) [Author and Title](#)

Mucha, S., Heinzlmeir, S., Kriegbaumer, V., Strickland, B., Kirchhelle, C., Choudhary, M., Kowalski, N., Eichmann, R., Huckelhoven, R., Grill, E., Kuster, B., and Glawischnig, E. (2019). The Formation of a Camalexin Biosynthetic Metabolon. *Plant Cell* 31, 2697-2710.

Pubmed: [Author and Title](#)

Google Scholar: [Author Only](#) [Title Only](#) [Author and Title](#)

Muller, T.M., Bottcher, C., Morbitzer, R., Gotz, C.C., Lehmann, J., Lahaye, T., and Glawischnig, E. (2015). TRANSCRIPTION ACTIVATOR-LIKE EFFECTOR NUCLEASE-Mediated Generation and Metabolic Analysis of Camalexin-Deficient *cyp71a12 cyp71a13* Double Knockout Lines. *Plant Physiol* 168, 849-858.

Pubmed: [Author and Title](#)

Google Scholar: [Author Only](#) [Title Only](#) [Author and Title](#)

Nadeau, J.A., and Sack, F.D. (2002). Control of stomatal distribution on the Arabidopsis leaf surface. *Science* 296, 1697-1700.

Pubmed: [Author and Title](#)

Google Scholar: [Author Only](#) [Title Only](#) [Author and Title](#)

Nafisi, M., Goregaoker, S., Botanga, C.J., Glawischnig, E., Olsen, C.E., Halkier, B.A., and Glazebrook, J. (2007). Arabidopsis cytochrome P450 monooxygenase 71A13 catalyzes the conversion of indole-3-acetaldoxime in camalexin synthesis. *Plant Cell* 19, 2039-2052.

Pubmed: [Author and Title](#)

Google Scholar: [Author Only](#) [Title Only](#) [Author and Title](#)

Niu, M.L., Huang, Y., Sun, S.T., Sun, J.Y., Cao, H.S., Shabala, S., and Bie, Z.L. (2018). Root respiratory burst oxidase homologue-dependent H2O2 production confers salt tolerance on a grafted cucumber by controlling Na+ exclusion and stomatal closure. *Journal of Experimental Botany* 69, 3465-3476.

Pubmed: [Author and Title](#)

Google Scholar: [Author Only](#) [Title Only](#) [Author and Title](#)

Ogawa, E., Yamada, Y., Sezaki, N., Kosaka, S., Kondo, H., Kamata, N., Abe, M., Komeda, Y., and Takahashi, T. (2015). ATML1 and PDF2 Play a Redundant and Essential Role in Arabidopsis Embryo Development. *Plant Cell Physiol* 56, 1183-1192.

Pubmed: [Author and Title](#)

Google Scholar: [Author Only](#) [Title Only](#) [Author and Title](#)

Ohashi-Ito, K., and Bergmann, D.C. (2006). Arabidopsis FAMA controls the final proliferation/differentiation switch during stomatal development. *Plant Cell* 18, 2493-2505.

Pubmed: [Author and Title](#)

Google Scholar: [Author Only](#) [Title Only](#) [Author and Title](#)

Peterson, K.M., Shyu, C., Burr, C.A., Horst, R.J., Kanaoka, M.M., Omae, M., Sato, Y., and Torii, K.U. (2013). Arabidopsis homeodomain-leucine zipper IV proteins promote stomatal development and ectopically induce stomata beyond the epidermis. *Development* 140, 1924-1935.

Pubmed: [Author and Title](#)

Google Scholar: [Author Only](#) [Title Only](#) [Author and Title](#)

Pillitteri, L.J., and Torii, K.U. (2012). Mechanisms of Stomatal Development. *Annu Rev Plant Biol* 63, 591-614.

Pubmed: [Author and Title](#)

Google Scholar: [Author Only](#) [Title Only](#) [Author and Title](#)

Pillitteri, L.J., and Dong, J. (2013). Stomatal development in Arabidopsis. *Arabidopsis Book* 11, e0162.

Pubmed: [Author and Title](#)

Google Scholar: [Author Only](#) [Title Only](#) [Author and Title](#)

Pillitteri, L.J., Sloan, D.B., Bogenschutz, N.L., and Torii, K.U. (2007). Termination of asymmetric cell division and differentiation of stomata. *Nature* 445, 501-505.

Pubmed: [Author and Title](#)

Google Scholar: [Author Only](#) [Title Only](#) [Author and Title](#)

Pilot, G., Lacombe, B., Gaymard, F., Cherel, I., Boucherez, J., Thibaud, J.B., and Sentenac, H. (2001). Guard cell inward K+ channel activity in arabidopsis involves expression of the twin channel subunits KAT1 and KAT2. *J Biol Chem* 276, 3215-3221.

Pubmed: [Author and Title](#)

Google Scholar: [Author Only](#) [Title Only](#) [Author and Title](#)

Pitzschke, A., Xue, H., Persak, H., Datta, S., and Seifert, G.J. (2016). Post-Translational Modification and Secretion of Azelaic Acid Induced 1 (AZI1), a Hybrid Proline-Rich Protein from Arabidopsis. *Int J Mol Sci* 17.

Pubmed: [Author and Title](#)

Google Scholar: [Author Only](#) [Title Only](#) [Author and Title](#)

Rajniak, J., Barco, B., Clay, N.K., and Sattely, E.S. (2015). A new cyanogenic metabolite in Arabidopsis required for inducible pathogen defence. *Nature* 525, 376-379.

Pubmed: [Author and Title](#)

Google Scholar: [Author Only Title Only Author and Title](#)

Rudall, P.J., Hilton, J., and Bateman, R.M. (2013). Several developmental and morphogenetic factors govern the evolution of stomatal patterning in land plants. *New Phytologist* 200, 598-614.

Pubmed: [Author and Title](#)

Google Scholar: [Author Only Title Only Author and Title](#)

Shanks, C.M., Hecker, A., Cheng, C.Y., Brand, L., Collani, S., Schmid, M., Schaller, G.E., Wanke, D., Harter, K., and Kieber, J.J. (2018). Role of BASIC PENTACysteine transcription factors in a subset of cytokinin signaling responses. *Plant J* 95, 458-473.

Pubmed: [Author and Title](#)

Google Scholar: [Author Only Title Only Author and Title](#)

Shpak, E.D., McAbee, J.M., Pillitteri, L.J., and Torii, K.U. (2005). Stomatal patterning and differentiation by synergistic interactions of receptor kinases. *Science* 309, 290-293.

Pubmed: [Author and Title](#)

Google Scholar: [Author Only Title Only Author and Title](#)

Simonini, S., and Kater, M.M. (2014). Class I BASIC PENTACysteine factors regulate HOMEOBOX genes involved in meristem size maintenance. *J Exp Bot* 65, 1455-1465.

Pubmed: [Author and Title](#)

Google Scholar: [Author Only Title Only Author and Title](#)

Simonini, S., Roig-Villanova, I., Gregis, V., Colombo, B., Colombo, L., and Kater, M.M. (2012). Basic pentacysteine proteins mediate MADS domain complex binding to the DNA for tissue-specific expression of target genes in *Arabidopsis*. *Plant Cell* 24, 4163-4172.

Pubmed: [Author and Title](#)

Google Scholar: [Author Only Title Only Author and Title](#)

Song, Y., Miao, Y., and Song, C.P. (2014). Behind the scenes: the roles of reactive oxygen species in guard cells. *New Phytol* 201, 1121-1140.

Pubmed: [Author and Title](#)

Google Scholar: [Author Only Title Only Author and Title](#)

Sugano, S.S., Shimada, T., Imai, Y., Okawa, K., Tamai, A., Mori, M., and Hara-Nishimura, I. (2010). Stomagen positively regulates stomatal density in *Arabidopsis*. *Nature* 463, 241-U130.

Pubmed: [Author and Title](#)

Google Scholar: [Author Only Title Only Author and Title](#)

Sun, X., Xu, D., Liu, Z., Kleine, T., and Leister, D. (2016). Functional relationship between mTERF4 and GUN1 in retrograde signaling. *J Exp Bot* 67, 3909-3924.

Pubmed: [Author and Title](#)

Google Scholar: [Author Only Title Only Author and Title](#)

Szyroki, A., Ivashikina, N., Dietrich, P., Roelfsema, M.R.G., Ache, P., Reintanz, B., Deeken, R., Godde, M., Felle, H., Steinmeyer, R., Palme, K., and Hedrich, R. (2001). KAT1 is not essential for stomatal opening. *P Natl Acad Sci USA* 98, 2917-2921.

Pubmed: [Author and Title](#)

Google Scholar: [Author Only Title Only Author and Title](#)

Takada, S., Takada, N., and Yoshida, A. (2013). ATML1 promotes epidermal cell differentiation in *Arabidopsis* shoots. *Development* 140, 1919-1923.

Pubmed: [Author and Title](#)

Google Scholar: [Author Only Title Only Author and Title](#)

Trapnell, C., Cacchiarelli, D., Grimsby, J., Pokharel, P., Li, S., Morse, M., Lennon, N.J., Livak, K.J., Mikkelsen, T.S., and Rinn, J.L. (2014). The dynamics and regulators of cell fate decisions are revealed by pseudotemporal ordering of single cells. *Nat Biotechnol* 32, 381-386.

Pubmed: [Author and Title](#)

Google Scholar: [Author Only Title Only Author and Title](#)

Underwood, W., Melotto, M., and He, S.Y. (2007). Role of plant stomata in bacterial invasion. *Cell Microbiol* 9, 1621-1629.

Pubmed: [Author and Title](#)

Google Scholar: [Author Only Title Only Author and Title](#)

Vanneste, S., Coppens, F., Lee, E., Donner, T.J., Xie, Z., Van Isterdael, G., Dhondt, S., De Winter, F., De Rybel, B., Vuylsteke, M., De Veylder, L., Friml, J., Inze, D., Grotewold, E., Scarpella, E., Sack, F., Beemster, G.T., and Beeckman, T. (2011). Developmental regulation of CYCA2s contributes to tissue-specific proliferation in *Arabidopsis*. *EMBO J* 30, 3430-3441.

Pubmed: [Author and Title](#)

Google Scholar: [Author Only Title Only Author and Title](#)

von Groll, U., and Altmann, T. (2001). Stomatal cell biology. *Current Opinion in Plant Biology* 4, 555-560.

Pubmed: [Author and Title](#)

Google Scholar: [Author Only Title Only Author and Title](#)

Xu, T., Nagawa, S., and Yang, Z. (2011). Uniform auxin triggers the Rho GTPase-dependent formation of interdigitation patterns in pavement cells. *Small GTPases* 2, 227-232.

Pubmed: [Author and Title](#)

Google Scholar: [Author Only Title Only Author and Title](#)

Xu, T., Wen, M., Nagawa, S., Fu, Y., Chen, J.G., Wu, M.J., Perrot-Rechenmann, C., Friml, J., Jones, A.M., and Yang, Z (2010). Cell surface- and rho GTPase-based auxin signaling controls cellular interdigitation in *Arabidopsis*. *Cell* 143, 99-110.

Pubmed: [Author and Title](#)

Google Scholar: [Author Only Title Only Author and Title](#)

Yoo, S.D., Cho, Y.H., and Sheen, J. (2007). *Arabidopsis* mesophyll protoplasts: a versatile cell system for transient gene expression analysis. *Nat Protoc* 2, 1565-1572.

Pubmed: [Author and Title](#)

Google Scholar: [Author Only Title Only Author and Title](#)

Zeng, W., Melotto, M., and He, S.Y. (2010). Plant stomata: a checkpoint of host immunity and pathogen virulence. *Curr Opin Biotechnol* 21, 599-603.

Pubmed: [Author and Title](#)

Google Scholar: [Author Only Title Only Author and Title](#)

Zhang, C., Mallery, E.L., and Szymanski, D.B. (2013). ARP2/3 localization in *Arabidopsis* leaf pavement cells: a diversity of intracellular pools and cytoskeletal interactions. *Front Plant Sci* 4, 238.

Pubmed: [Author and Title](#)

Google Scholar: [Author Only Title Only Author and Title](#)

Zhang, D., Tian, C., Yin, K., Wang, W., and Qiu, J.L. (2019). Postinvasive Bacterial Resistance Conferred by Open Stomata in Rice. *Mol Plant Microbe Interact* 32, 255-266.

Pubmed: [Author and Title](#)

Google Scholar: [Author Only Title Only Author and Title](#)

Zhang, J.Y., He, S.B., Li, L., and Yang, H.Q. (2014). Auxin inhibits stomatal development through MONOPTEROS repression of a mobile peptide gene STOMAGEN in mesophyll. *P Natl Acad Sci USA* 111, E3015-E3023.

Pubmed: [Author and Title](#)

Google Scholar: [Author Only Title Only Author and Title](#)

Zhou, Y., Zhou, B., Pache, L., Chang, M., Khodabakhshi, A.H., Tanaseichuk, O., Benner, C., and Chanda, S.K. (2019). Metascape provides a biologist-oriented resource for the analysis of systems-level datasets. *Nat Commun* 10, 1523.

Pubmed: [Author and Title](#)

Google Scholar: [Author Only Title Only Author and Title](#)